UNIVERSITY OF KWAZULU-NATAL ™

INYUVESI YAKWAZULU-NATALI

FUSARIC ACID AND FUMONISIN B_1 CO-TREATMENT REGULATES AMPK SIGNALLING AND INDUCES APOPTOSIS IN HEPG2 CELLS.

by

Ms. PATANE SYLVESTER SHILABYE

BSc in Medical Sciences (Hons) (University of Limpopo)

Submitted in fulfillment of the requirements for the degree

MASTER OF MEDICAL SCIENCES

in the

Discipline of Medical Biochemistry and Chemical Pathology

School of Laboratory Medicine and Medical Sciences

College of Health Sciences

UNIVERSITY OF KWAZULU-NATAL

Durban

SUPERVISOR: Prof A.A. Chuturgoon

CO-SUPERVISOR: Ms. T. Ghazi

2019

DECLARATION

I, Patane Sylvester Shilabye, hereby declare that the research presented in this thesis is my own, and apart from normal content and technical guidance from supervisors and senior colleagues, no other assistance was sought and/or received. Neither the substance nor any part of this thesis has been submitted in the past, or is being, or is to be submitted for a degree in this or any other University. I further declare that all information from other sources has been duly referenced and acknowledged in accordance.

The research described in this study was carried out in the Discipline of Medical Biochemistry, School of Laboratory Medicine and Medical Science, College of Health Sciences, University of Kwa-Zulu Natal, under the supervision of Professor A.A. Chuturgoon and Ms. T. Ghazi.

Signature: 

Date:10/12/2019

DEDICATION

I dedicate my research report work to my family and all those who supported me on this academic journey, I will always appreciate all they have done. Most of all I dedicate this research dissertation to the almighty Lord for His grace, mercy and guidance.

ACKNOWLEDGEMENTS

To all my loved ones and family, particularly my parents Mr. P.L and Mrs. F.M Shilabye, my sister (Miss N.O Shilabye,) and Mr. Phalane E.U.M., I would like to thank you guys for the support you have given to me. You have all supported my decision to come and study at UKZN which is quite distant from home, and you kept on supporting me throughout the year. You may not be at KZN to support me physically, but you have given me more emotional support when I needed it most. I will forever appreciate you guys and your words of wisdom and encouragement.

Prof A.A Chuturgoon

I am honoured to have been under your supervision and would always do it all over again given a chance. I am particularly grateful for accepting me in your research group even when you did not know me, my skills, my experience, or my passion thereof. I am glad my research work was in unfamiliar toxicology, a field that I have greatly enjoyed venturing into and learned a lot from. This current study is important to me as I have always lived in places where maize is the staple food, hence was important to learn about these mycotoxins. Thank you for your guidance.

Terisha Ghazi

Thank you for helping and guiding me with the laboratory work and being available whenever I needed your assistance. For someone who was doing tissue culture for the 1st time like me, it was not so difficult to master and that's because I had you to guide me. I also appreciate your help during the stressful times of thesis time, taking off time from your busier schedule. You are an amazing and patient co-supervisor.

Thilona

To Thilona, you are the best western blot teacher I have ever met I managed to do western blot and I believe I learned a lot of troubleshooting skills to carry me through, thanks to your guidance and patience with me. I am more grateful because you helped me with my work even though you had your own to do.

Fellow master's students

Class of 2019, I appreciate your help and pieces of advice when I needed those.

Ashmika

Thank you for everything buddy. I consider our joining the department at the same time a very beautiful fateful coincidence as you had become very helpful and supportive to me. Thank you for being such a good friend, all-round.

National Research Foundation (NRF) and College of Health Sciences

Scholarships and Funding

PRESENTATIONS

Fusaric Acid and Fumonisin B_1 Co-treatment Triggers Apoptosis in HepG2 cells.

Shilabye P.S., Ghazi T. and Chuturgoon A.A.

Laboratory Medicine and Medical Sciences (LMMS) Research Symposium (6th September 2019), University of Kwa-Zulu Natal, Durban, South Africa.

Table of Contents

LIST OF FIGURES

CHAPTER 2:

CHAPTER 3:

CHAPTER 4:

APPENDICES

LIST OF TABLES

CHAPTER 3

APPENDICES

ABBREVIATIONS

$2^{-\Delta\Delta Ct}$	Fold change
ADP	Adenosine diphosphate
AIP	Aryl hydrocarbon receptor-interacting protein
AMP	Adenosine monophosphate-activated protein kinase
AMP	Adenosine monophosphate
Apaf-1	Apoptotic protease activating factor 1
ATP	Adenosine triphosphate
BCA	Bicinchoninic acid
BAK	BCL-2 antagonist killer 1
BAX	Bcl-2-associated X protein
BCL-2	B-cell lymphoma 2
BCL-XL	B-cell lymphoma-extra large
BHT	Butylated hydroxytoluene
BID	BH3 interacting-domain death agonist
BIM	BH3 interacting-domain death agonist
BSA	Bovine serum albumin
CCM	Complete culture media
CDKI	Cyclin-dependent kinase inhibitor
cDNA	Complementary DNA
CT	Threshold cycle
DISC	Death-inducing signalling complex
DMSO	Dimethyl sulfoxide
dNTP	Deoxynucleoside triphosphate
DR3-6	Death receptor 3-6

CBS domain	Cystathionine-beta-synthase
EMEM	Eagle's Essential Minimal Media
ER	Endoplasmic reticulum
FA	Fusaric acid
FADD	Fas-associated protein with death domain
Fas/Fas L	Fatty acid synthase/ Fatty acid synthase ligand
FB_1	Fumonisin B_1
FOXO3a	Forkhead box class O 3a
GAPDH	Glyceraldehyde 3-phosphate dehydrogenase
H_2O_2	Hydrogen peroxide
H_3PO_4	Phosphoric acid/ orthophosphoric acid
HCl	Hydrochloric acid/ Hydrogen chloride
HepG2	Human hepatoma G2
HRP	Horse radish peroxidase
Hrs	Hours
IC_{50}	Inhibitory concentration of 50%
LDH	Lactate dehydrogenase
MAPK	Mitogen-activated protein kinase
MCL-1	Myeloid cell leukemia-1
MDA	Malondialdehyde
Mg^{2+}	Magnesium ion
MiR124	MicroRNA-124
MTT	3- (4,5-dimethylthiazol-2-yl)-2,5-diphenyl tetrazolium bromide
NF-κB	Nuclear factor kappa B
NAD^+	Nicotinamide adenine dinucleotide
NADH	Nicotinamide adenine dinucleotide phosphate

O_2	Oxygen
p-AMPK	Phosphorylated Adenosine monophosphate-activated protein kinase
PARP	Poly-ADP ribose polymerase
PBS	Phosphate-buffered saline
PRKAA1-2	Protein kinase AMP-activated catalytic subunit alpha 1
PRKAB1-2	Protein kinase AMP-activated non-catalytic subunit beta 1
PRKAG1-3	Protein kinase AMP-activated non-catalytic subunit gamma 1
qPCR	Quantitative polymerase chain reaction
RNA	Ribonucleic acid
ROS	Reactive oxygen species
SDS	Sodium dodecyl sulphate
SDS-PAGE	Sodium dodecyl sulphate polyacrylamide gel electrophoresis
TBA	Thiobarbituric acid
TBARS	Thiobarbituric acid-reactive substances
TCA	Tricarballylic acid
TDA1	Transactivation domain 1
TDA2	Transactivation domain 2
TEMED	Tetramethylethylenediamine
Thp-1	Human monocytic leukemia cells
TNFR1	Tumour necrosis factor-receptor 1
TRAIL	Tumour necrosis factor-related apoptosis-inducing ligand
Tris	Tris(hydroxymethyl) aminomethane
Tris-HCl	Tris (hydroxymethyl) aminomethane hydrochloric acid
TTBS	Tween 20-Tris buffered saline

ABSTRACT

Background/Aim: Fusaric acid (FA) and Fumonisin B_1 (FB_1) are mycotoxins produced by *Fusarium* fungal species. These mycotoxins are major contaminants of maize and contribute to toxicity in animals and humans. The main mechanisms of FA and FB_1 toxicity involve the induction of oxidative stress and apoptosis; however, FA was additionally found to chelate divalent cations, whereas FB_1 inhibits sphingolipid synthesis. AMPK is an energy sensor involved in regulating cell proliferation. AMPK targets the transcription factors, p53 and FOXO3a that play a major role in apoptosis. To date numerous studies have investigated the individual effects of FA and FB_1, however, their combined synergistic effects are unclear. This study investigated the effect of FA and FB_1 co-treatment on AMPK-induced apoptosis in liver HepG2 cells.

Methods: HepG2 cells were cultured and co-treated with various concentrations (5, 27, 100μM and combined 104μM FA and 200μM FB_1 IC_{50}s) of FA and FB_1 for 24 hrs. Cytotoxic effects of FA and FB_1 on HepG2 cells were determined using the MTT assay. The TBARS assay was used to determine oxidative stress. Western blot was used to determine protein expression of AMPK, p-AMPK and p53, whereas q-PCR was used to measure *FOXO3a* mRNA expression. LDH assay was used to measure membrane integrity. ATP levels and activity of caspases -3/7, -8 and -9 were measured using luminometry.

Results: A combination of FA and FB_1 decreased cell viability in a dose dependant manner. An IC_{50} of 27μM for FA and FB_1 was obtained. ATP levels were significantly increased at 5μM and 27μM, whereas at 100μM and combined IC_{50}s were significantly decreased (*p<0.0001*). Oxidative stress was significantly increased in FA and FB_1 treated cells in a dose dependent manner (*p<0.0001*). The protein expression of total AMPK was decreased at 5μM, but increased at 27μM, 100μM and combined IC_{50}s in relation to control (*p<0.0001*). p-AMPK showed a significant decrease (*p<0.0001*) in all FA and FB_1 treated samples despite the increase in the expression of total AMPK. *FOXO3a* mRNA expression was decreased at 5μM and at combined IC_{50}s, with the decrease being significant at 5μM. The results also indicated an increase at 27μM and 100μM (*p<0.0001*). p53 protein expressions were significantly decreased in all samples (*p<0.0001*). Caspase -3/7, -8 and -9 were significantly increased at 5-100μM and decreased at combined IC_{50}s in HepG2 cells. In FA and FB_1 samples, LDH levels were significantly decreased at 5μM and 27μM, and significantly increased at 100μM and combined IC_{50}s (*p<0.0001*).

Conclusion: FA and FB_1 co-treatments suppressed AMPK signalling by downregulating p-AMPK and induced apoptosis and/necrosis in HepG2 cells.

CHAPTER 1: INTRODUCTION

Mycotoxins are toxic secondary metabolites synthesised by fungi that cause diseases and death in humans and animals (Venkatesh, et al., 2019). Fusaric acid (FA) and Fumonisin B_1 (FB_1) are mycotoxins co-produced by *Fusarium* species such as *Fusarium verticillioides* (Bacon et al., 1996; Shi, et al.,2017). These mycotoxins are found on maize and other corn-based foods in low (<100 µg/kg) to high concentrations (>500 µg/kg) (Bacon, et al., 1996); and consumption of contaminated foods have been shown to cause toxicity in various organ systems such as the brain, liver, and kidneys in animals and humans (Rong, et al., 2018). FA is a chelating agent and its ability to remove essential metal ions plays a major role in inducing toxicity (Bacon et al., 1995). FA increases the toxicity of other *Fusarium* mycotoxins such as Trichothecenes, zearalenone, fumonisins, and enniatins (Yabuta et al., 1937; Han, et al., 2014). FB_1 is a member of Fumonisin family. It is similar to the sphingoid bases in terms of its structure; therefore, allowing this mycotoxin to interact with the sphinganine binding site. The ability of FB_1 to bind to the enzyme ceramide synthase, enables it to prevent the formation of ceramide by blocking ceramide synthase (Blacutt, et al., 2017). Additionally, FB_1 has been associated with neural defects and oesophageal cancer in humans and animals (Yuan, et al.,2019). The tolerated daily dose of FB_1 in humans is 2 to 4 µg/kg and <100µg/kg for animals (Bryden, 2011). There is currently no maximum daily tolerable dose for FA, and this puts humans and animals at a high risk of exposure and toxicity.

Adenosine monophosphate-activated protein kinase (AMPK) is an energy sensor; however, it is proposed as an apoptotic molecule in human cancer cells (Kim, et al., 2007). AMPK can be activated by multiple factors such as oxidative stress, ATP depletion, and hypoxia (Rehman, et al., 2014). Oxidative stress occurs when there is an imbalance between reactive oxygen species (ROS) and antioxidants, in favour of the former. Mycotoxins induce overproduction of ROS and deplete antioxidant levels, thereby, causing oxidative stress (Pizzino, et al., 2017). Oxidative stress can activate AMPK directly by oxidising cysteine residues of AMPK and indirectly through an AMP-mediated pathway (Jeon, et al., 2016). Once activated, AMPK can activate or inhibit oncogenes and tumour suppressor proteins by either initiating or preventing its phosphorylation. AMPK directly phosphorylates and activates the transcription factor, *FOXO3a* which plays an important role in tumour suppression pathways (Zhang, et al., 2011). In stressed cells, the activation of *FOXO3a* leads to apoptosis (Yang, et al., 2016).

Apoptosis refers to programmed cell death which is carried out by caspases (Walsh, et al., 2008). *FOXO3a* induces the expression of numerous pro-apoptotic associates of the Bcl-2 family of proteins, stimulates Fas ligand and TNF-related apoptosis-inducing ligand, and it increases the level of cyclin-dependent kinase inhibitors (CDKIs); therefore, inhibiting cell growth and inducing apoptosis (Zhang, et al., 2011). In apoptosis induced via the AMPK-p53 pathway, p53 regulates the initiation of apoptosis by transactivating the pro-apoptotic molecules, BAX and BIM, and inhibits anti-apoptotic members (Su, et al., 2015). p53 is a tumour suppressor protein that functions to regulate cell cycle arrest and apoptosis in response to cellular stress. p53 can induce both intrinsic and extrinsic pathways of apoptosis.

1.1 PROBLEM STATEMENT

FA and FB_1 are mycotoxins produced by *Fusarium* species that commonly contaminate maize and other agricultural foods. These foods are an essential component of the staple diet in developing countries, especially those populations residing in rural and poverty-stricken areas. These mycotoxins are often co-produced and contribute to toxicity in both animals and humans. Currently, there are limited studies determining the combined effect of FA and FB_1 in humans and evaluating any possible toxic effects will be beneficial in developing therapeutic interventions against FA and FB_1 toxicity.

1.2 RESEARCH QUESTION

Does FA and FB_1 induce a toxic synergistic effect in HepG2 cells?

What is the molecular mechanism underlying the effect of FA and FB_1 co-treatment in HepG2 cells?

1.3 AIM

To determine the effect of FA and FB_1 co-treatment on AMPK signalling and apoptosis in human liver (HepG2) cells.

1.4 HYPOTHESIS

FA and FB_1 regulates AMPK and induces apoptosis by elevating oxidative stress in HepG2 cells.

1.5 OBJECTIVES

- To investigate the effect of FA and FB_1 co-treatment on AMPK induced apoptosis in HepG2 cells using western blots and real-time PCR
- To investigate the effects of FA and FB_1 co-treatment on co-treating with FA and FB_1 on HepG2 cells after 24 hours of exposure
- To investigate the effects of FA and FB_1 co-treatment on oxidative stress using TBARS assay
- To investigate the effects of FA and FB_1 co-treatment on apoptosis in HepG2 cells by assessing caspase (8,9 and 3/7) activities and ATP levels using Luminometry assay.
- To investigate the effects of FA and FB_1 co-treatment on AMPK signalling using real-time PCR and western blots.

CHAPTER 2: LITERATURE REVIEW

2.1 Mycotoxins

Mycotoxins are toxic secondary metabolites produced by fungi and molds that commonly contaminate agricultural foods and are potential threats to human and animal health worldwide (Rong, et al., 2018; Venkatesh, et al., 2019). The most common food-borne fungi belong to the genera *Fusarium*, *Alternaria*, *Aspergillus*, and *Penicillium*. These fungal species are capable of producing various mycotoxins such as fumonisins, aflatoxin, ochratoxin, deoxynivalenol, and T2-toxin.

Improper storage and transportation from pre-harvest to post-harvest can result in fungal growth and mycotoxin accumulation on various agricultural crops (Rong, et al., 2018). They are regularly found in regions favourable for mold growth and those with hot and humid climate (Zain, 2011). Mycotoxins are biologically active, and their biological activity differs according to their chemical structures (Rong, et al., 2018). Exposure to mycotoxins can occur via ingestion, inhalation, and dermal routes. Mycotoxins induce oxidative stress, cytotoxicity or genotoxicity. They cause toxicity in vital organs such as the liver and kidneys (Zain, 2011).

Fig 2.1: *Fusarium* mycotoxin contaminated maize (Driehuis, 2011).

2.1.1 *Fusarium* species

The *Fusarium* species are soil-borne fungi that produce various potent mycotoxins. Several plants are symptomatically and asymptomatically infected by the *Fusarium* species (Brown,

et al., 2012). It is a major fungal genus associated with maize in African continents and it comprises of various toxigenic species including *F. verticillioides and F. proliferatum*. These species are frequently found in rural areas and poverty-stricken areas that have inadequate food storage methods (Fandohan, et al., 2003*).*

2.1.2 Fusaric acid

Fusaric acid (FA; 5-butylpicolinic acid) is a secondary metabolite and mycotoxin produced by *Fusarium* species including *Fusarium verticilloides, oxysporum, heterosporium*, etc. It is the first mycotoxin to be isolated and was originally isolated from *Fusarium heterosporium* (López-Díaz, et al., 2017). During infection, FA accumulates in maize and other agricultural foods (Rani, et al., 2009). According to Bacon et al., (1995), FA was found to contaminate maize in low (<100 µg/g) and high concentrations (>500 µg/g), however, this depends on the type of *Fusarium* species synthesising the mycotoxin.

FA is a chelating agent and the removal of essential divalent metal ions has been shown to cause toxicity in both plants and animals (Bacon et al., 1995, Yin, et al., 2015; López-Díaz, et al., 2018). This host non-specific mycotoxin also increases the overall toxicity of other co-produced *Fusarium* mycotoxins including fumonisins, zearalenone and trichothecenes (deoxynivalenol and nivalenol) (Ali, *et al.*, 1998; Rani, et al., 2009; Han, et al., 2014).

2.1.2.1 Fusaric acid structure

FA is a picolinic acid derivative that contains a pyridine ring and a 5-butyl side chain. The butyl chain enables FA to permeate lipid rich cell membranes and enter the cell (Fernández-Pol, 1998; Ogata. et al., 2001; Stack, et al., 2014). The pyridine ring enables FA to form chelates by sequestering divalent cations between its N-atom and carboxyl radical in the α-position (Gäumann, 1958; Mehrotra, 2013). FA also contains a hydroxyl group (OH^-) that gives FA it's weak acid properties. Due to its weak acid properties, FA can disrupt the hydrogen gradient across the mitochondrial membrane (Bochner, et al., 1980; Crutcher, et al., 2017).

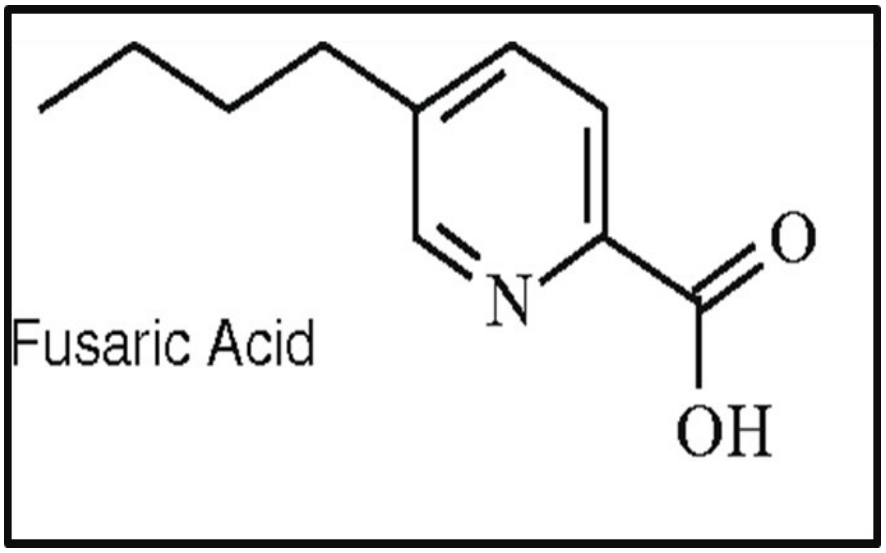

Fig 2.2: Fusaric acid structure (Crutcher, et al., 2014).

2.1.2.2 Toxic effects and mechanism of action of Fusaric acid

At subcellular level, fusaric acid's toxicity results in membrane dysfunctions, membrane potential alterations, elevating electrolyte leakage, respiratory activity inhibitions moreover, decreasing ATP levels through disturbing the electrochemical gradients for hydrogen and potassium ions at the plasma membrane thus resulting in membrane depolarisation (Pavlovkin, et al., 2003; Singh, et al., 2016). Fusaric acid is also believed to be involved in fungal pathogenesis through reducing cell viability (Singh, et al., 2016). According to a study by Rani, et al., (2009), FA induces ROS production.

FA induces hepatotoxicity by impairing mitochondrial function and biogenesis (Abdul, et al., 2016). FA is immunotoxic to peripheral blood mononuclear cells and Thp-1 cells by altering the MAPK signalling pathway (Dhani, et al., 2017). FA was also shown to induce genotoxicity and cytotoxicity in HepG2 cells by altering global and promoter DNA methylation (Ghazi, et al., 2019). FA elevates ROS production which reacts with various cellular components thus causing oxidative damage to nucleic acids, proteins, and lipids of cellular membranes. Damage to cellular macromolecules eventually leads to cellular dysfunction and cell death (Singh, et al., 2014). Other studies have shown that FA causes notochord malformation in zebrafish embryos through copper chelation from the active site of lysyl oxidase (Yin, et al., 2015), bone ossification and growth delay on mice foetus by chelating calcium (Reddy, et al., 1996; Yin, et al., 2015; Gruber-Dorninger, et al., 2017).

2.1.3 Fumonisin B_1

Fumonisin B_1 (FB_1) is a member of the fumonisin family and is a hydrophilic secondary metabolite predominantly synthesised by *Fusarium verticillioides* and *Fusarium proliferatum* (Voss, et al., 2013; Yuan, et al., 2019). These mycotoxins contaminate agricultural foods and can induce toxicity in animals and humans. FB_1 is the most commonly studied member of the fumonisin family (Yuan, et al., 2019), and compared to the other fumonisins, FB_1 has been shown to be produced in the highest quantities with the strongest toxicity (Yuan, et al., 2019). The concentrations of FB_1 are extremely high in South Africa (11,000 µg/kg), Thailand (18,800 µg/kg) and China (25,970 µg/kg) for compound feed and maize (Bryden, 2011). According to the food and agriculture organization (FAO), the tolerated quantity that human can consume is 2 to 4 µg/kg per day, whereas animals' tolerance is much higher, which is up to 100 mg/kg (Yuan, et al.,2019). FB_1 is stable under normal cooking and food processing techniques (Blacutt, et al., 2017).

2.1.3.1 Fumonisin B_1 structure

The structure of FB_1 consists of a long (19-20) carbon aminopolyhydroxyalkyl chain (Wu, et al., 2019). FB_1 is a diester of propane-1,2,3-tricarboxylic acid (TCA) and 2-amino-12,16-dimethyl-3,5,10,14,15-pentahydroxyeicosane, in which the carbon 14 (C14) and C15 hydroxyl groups are esterified with a terminal carboxyl group of TCAs (Voss, et al., 2007). FB_1 structure consists of a free amino group at C1 and the primary amino group at C2. These amino groups are crucial for fumonisin B biological activities (Voss, et al., 2007; Stockmann-Juvala, et al., 2008; Voss, et al., 2013). The fumonisin B contains C1 terminal methyl group A (Blacutt, et al., 2017). FB_1 is structurally similar to the sphingoid bases, sphinganine and sphingosine. Sphinganine is a precursor molecule required to produce ceramide (Blacutt, et al., 2017).

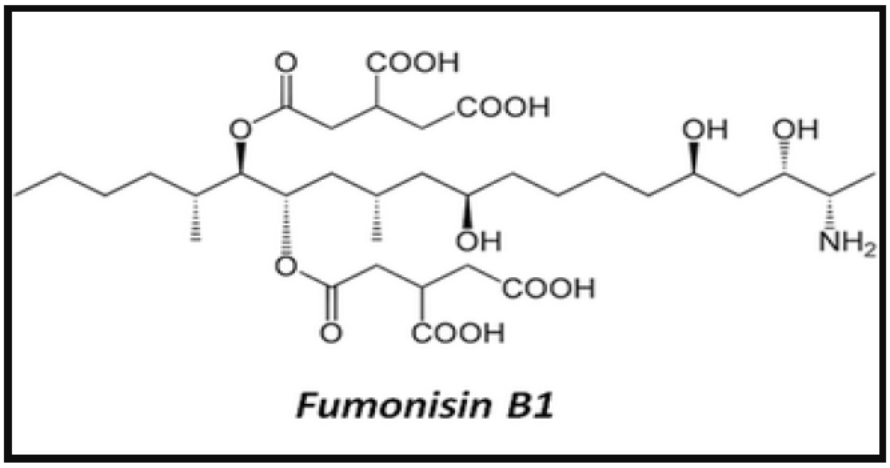

Fig 2 3: Structure of FB_1 (Zain, et al., 2011).

2.1.3.2 Fumonisin B_1: Mechanism of action

FB_1 is a known cause of hepatotoxicity, nephrotoxicity, and neurotoxicity in animals (Voss, et al., 1990, Mathur, et al., 2001). Other effects of FB_1 include apoptosis, oxidative stress, and inflammation (Stockmann-Juvala, et al., 2004). In humans, FB_1 is suspected to be a major cause of oesophageal cancer and neural tube defects (Yuan, et al., 2019). These disorders are identified in populations consuming excess quantities of contaminated corn-based food as their staple diet (Voss, et al., 2013). However, in animals, extreme consumption can result in severe damage in most organ systems (Yuan, et al., 2019).

The mechanism of FB_1 induced cellular toxicity involves inhibition of an enzyme called ceramide synthase (Blacutt, et al., 2017). FB_1 uses its aminopentol backbone of FB_1 which acts as both the inhibitor as well as a substrate of ceramide synthase thus preventing the production of ceramide. In the absence of FB_1 exposure, ceramide synthase is involved in the process where sphinganine is formed, thereafter, acetylated into dihydroceramide and ceramide (Stockmann-Juvala, et al., 2008). Inhibition of ceramide synthase results in elevated levels of sphingoid bases, sphinganine and sphingosine at the lesser degree (Merrill, et al., 2001). FB_1 also intensifies oxidative stress by suppressing glutathione activities while increasing malondialdehyde concentrations (Yuan, et al., 2019). FB_1 has been implicated in liver carcinogenesis (Blacutt, et al., 2017). This mycotoxin induces global DNA hypomethylation and histone demethylation, modulates microRNA (miR-27b) expression and increases AIP protein family (BIRC8/ILP-2) expressions (Chuturgoon, et al, 2014).

A recent study by Yuan et al., (2019) indicated that FB_1 reduces the viability of cells (pig iliac endothelium cells and HepG2 cells) in a dose-dependent manner by elevating ROS

production, this was proven by Methyl thiazolyl tetrazolium (MTT) and malondialdehyde (MDA) assays where cells had elevated levels of lipid peroxidation by-product called MDA. Singh and Kang, (2017) further report that after 24 hours FB_1 treatment, AMPK and Bcl-2 expressions were highly increased in HepG2 cells and mice liver cells. The study further explains that after 12 hours of treatment, both cells showed an increase in cytochrome c and caspase 3 activities, however, after 24 hours the HepG2 cells showed a decrease in both cytochrome c and caspase 3. The liver cells of mice showed a significant decrease after 4 days treatment with FB_1. Another study by Kim, et al., (2018), showed that the pro-apoptotic molecules, p53, caspase 9 and 3 were significantly increased in FB_1 treated cells. Although there are few studies on AMPK and FB_1, no studies have been conducted following co-treatment with FA and FB_1 on the AMPK pathway.

2.2 Oxidative stress

Oxidative stress is defined as an increase in intracellular ROS that can lead to damaged DNA, proteins, lipids, and cell death (Schieber, et al., 2015). Oxidative stress occurs as a result of cellular overproduction of oxygen radicals which overwhelms the cell's antioxidant capacity leading to an imbalance between ROS and the antioxidant defense (Pizzino, et al., 2017). ROS are products of aerobic metabolism, xenobiotics, cytokines as well as bacterial invasions (Ray, et al., 2012; Schieber, et al., 2015). ROS includes superoxide anion, hydrogen peroxide, and oxidative radicals. These by-products contain chemical properties that confer reactivity to different biological targets (Schieber, et al., 2015). The antioxidant defense is the protection mechanism used by cells to protect the biological system from free radical toxicity by combatting ROS (Patlevič, et al., 2016). The defense mechanism of antioxidants involves 3 steps; prevention, interception, and repair (Sies, et al., 1993). Antioxidant enzyme superoxide dismutase reduces toxic superoxide anions into H_2O_2, which will further be metabolised into H_2O and O_2 by catalase and glutathione peroxidase (Liu, et al., 2006).

2.3 AMPK and its structure

AMP-activated protein kinase (AMPK) refers to serine/threonine-protein kinase that acts as a sensor of cellular homeostasis (Harmel, et al., 2014). It is highly conserved across most eukaryotic organisms (Sanli, et al., 2014). AMPK exists as heterotrimer and consists of two catalytic α, two regulatory β and three regulatory γ subunits. These 7 subunit isoforms are encoded by separate genes, protein kinase AMP-activated catalytic subunit alpha 1-2

(*PRKAA1-2*), protein kinase AMP-activated non-catalytic subunit beta 1-2 (*PRKAB1-2*), and protein kinase AMP-activated non-catalytic subunit gamma 1-3 (*PRKAG1-3*), (Hardie, 2013). These 7 subunit isoforms yield 12 possible heterotrimeric complexes (Sanli, et al., 2014). AMPK α subunits are encoded by *PRKAA1 or PRKAA2* and located within different cellular compartments: AMPK-α1 is found in the cytoplasm whereas AMPK-α2 is found in the nucleus. AMPK-α1 controls signalling pathways and AMPK-α2 regulates gene transcription and expression (Harmel, et al., 2014). The beta subunits support binding of both α and γ subunits, which results in the formation of the AMPK-αβγ complex. Beta subunits also play a major role in regulating carbohydrate-binding module mediated-enzyme activity effects (Sanli, et al., 2014).

The gamma subunit comprises of 3 sites that can bind to adenine nucleotides and confer the ability of the kinase to act as an energy sensor (Hardie, 2013). The two sites contain Bateman domains that bind either ATP or AMP and the third site is tightly bound to AMP, without exchange (Richter and Ruderman, 2009). A study by Kim, et al. (2016), illustrated that the gamma subunit has a 4th site and that all 4 sites contain the cystathionine-β-synthase domain (CBS domain) also known as, Bateman domains. These 4 sites are numbered from 1-4 and this depends on the number of Bateman domain repeat carrying a conserved aspartate residue involved in the ligand binding. The gamma subunits of mammals second site do not bind to AMP or ATP, the fourth site is tightly bound to AMP, whereas the remaining regulatory sites, binds to either of the 3-adenine nucleotides (AMP, ADP or ATP). The first site plays a role in allosteric activation of AMPK when AMP binds to it, while the third site regulates the phosphorylation state at THR-172.

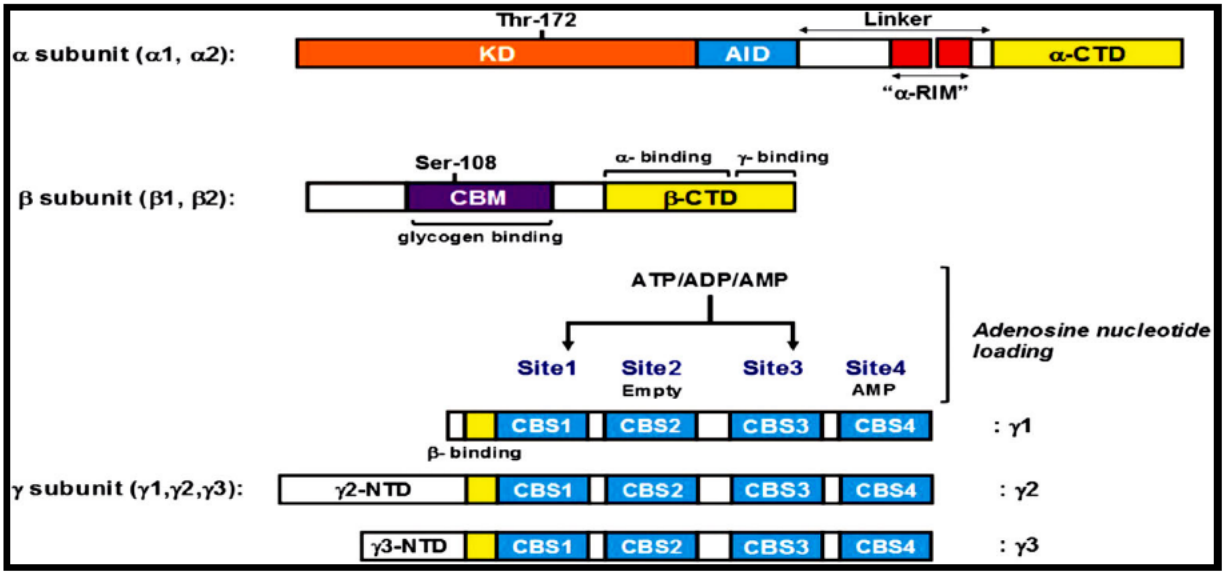

Fig 2.4: AMPK structure (Kim, et al., 2016).

2.3.1 AMPK activation

The activation of AMPK is heterogeneous in different tumour cells. It can either be tumour suppressive or oncogenic. Upon activation, AMPK can inhibit the propagation of tumour cells by causing cell cycle arrest and apoptosis (Zadra, et al., 2015). AMPK functions at both the physiological and molecular level. At a physiological level, reduced AMPK levels are linked to various metabolic disorders such as diabetes and obesity, whereas at the molecular level, the function of AMPK is associated with controlling cell proliferation and death through several cell signalling pathways (Rehman, et al., 2014). AMPK is allosterically activated via phosphorylation of its catalytic subunit's as well as binding of ADP to the regulatory subunits. Activated AMPK inhibits energy-consuming pathways such as fatty acid, carbohydrate, and protein synthesis, whereas energy-producing processes such as oxidative metabolism and mitochondrial biogenesis are initiated (Park, et al., 2018). The energy/ATP status has a crucial role in both cell proliferation and cell death; a decrease in ATP levels leads to the activation of AMPK and vice versa. In liver cells, short term deprivation of ATP can result in cell survival, however, prolonged deficiency of ATP triggers apoptosis (Kim, et al., 2007).

AMPK can also be activated by multiple factors including metabolic and cellular stresses which results in ATP depletion, pathological stress (for instance oxidative stress, hypoxia), hormones and cytokines (Rehman, et al., 2014). Activation of AMPK via ROS in stressed cells can result in apoptosis (Cardaci, 2012).

2.3.1.1 AMPK activations through pathological stress, oxidative stress

Cellular AMPK is activated in cells experiencing oxidative stress through the classical AMP-mediated pathway. ROS including hydrogen peroxides (H_2O_2) alters the AMP-ATP ratio by increasing AMP, therefore leading to the activation of AMPK through AMP-mediated/dependent pathway (Auciello, et al, 2014). Recent studies have indicated that AMPK can be activated by elevated ROS despite the absence of ATP. Oxidative stress controls the activity of AMPK by directly oxidising AMPK cysteine residues (Jeon, 2016). H_2O_2 stimulates AMPK through oxidative modifications, for instance; *S*-glutathionylation of the α and β subunits (Zmijewski, et al., 2010).

2.3.2 AMPK role as an antiproliferative molecule

The AMPK pathway has been implicated in cancer regulation. It is proposed as an apoptotic molecule and its activation has been related to both the initiation and execution of apoptosis

(Kim, et al., 2007). Activated AMPK has tumour suppressive effects by preventing oncogene phosphorylation and activation as well as phosphorylating and activating tumour suppressor genes such as p53, p21 and FOXO3a (El-Masry, et al., 2015; Wang, et al., 2017).

2.3.2.1 Apoptosis triggered via AMPK-FOXO3a pathway.

AMPK is a pro-survival kinase involved in the induction of apoptosis through various pathways including AMPK-FOXO3a pathway. It phosphorylates FOXO3a and induces its transcriptional activity (Yun, et al., 2014). The phosphorylation occurs on Ser626 of FOXO3a in the conserved region 3 (CR3) domain and this increases the binding of CBP/p300 as well as the transactivational activity of FOXO3a (Wang, et al., 2017). The AMPK -FOXO3a signalling pathway leads to the initiation of pro-apoptotic Bcl-2-family protein, Bcl-2 Interacting Mediator of cell death (BIM) (Cardaci, et al., 2012). BIM is responsible for initiating apoptotic cell death under physiologic and pathologic conditions (Shukla, et al., 2013). It is one of the initiators and orchestrators of apoptosis collectively known as BH3-only proteins (Frank, et al., 2015). To initiate apoptosis, these proteins directly activate Bcl-2-associated X protein (BAX) and BCL-2 antagonist killer 1 (BAK), while suppressing the anti-apoptotic proteins at the mitochondria and endoplasmic reticulum (Shamas-Din, et al.,2010).

2.3.2.1.a FOXO3a

FOXO3a is a member of the FOXOs subfamily. FOXO3a gene is located on chromosome 6q21 (Lui, et al., 2018). FOXOs are involved in various cellular processes such as cell differentiation, cell growth, survival, cell cycle, metabolism, stress and cell death (Zhang, et al., 2011). FOXOs are required to maintain the balance between cell death and proliferation (Yao, et al., 2017). In stress-exposed cells, the activation of FOXO3a triggers an apoptotic response (Yang, et al., 2016, Hesham et al., 2016) by inducing the expression of numerous pro-apoptotic associates of the BCL-2-family, stimulating the expression of death receptor ligands (fas ligand and tumour necrosis factor-related apoptosis-inducing ligand), and enhancing the levels of CDKIs in order to induce cell growth inhibition and apoptotic signalling (Zhang, et al., 2011; Das, et al., 2012). BCL-2-family members (BAX, BAK, BCL-2, BCL-XL, MCL-1, BID, and BIM) regulates the release of cytochrome C by regulating the permeability of the mitochondrial membrane (Su, et al., 2015).

2.3.2.2 Apoptosis induced through AMPK-p53 pathway.

The activation of AMPK also initiates apoptosis by inducing phosphorylation of p53 at serine 15 (Jones, et al., 2005). Upon phosphorylation/activation by AMPK, p53 regulates apoptosis by transactivating BID, BIM and BAX, and suppressing anti-apoptotic members such as BCL-2, BCL-XL and MCL-1 (Fridman, et al., 2003; Su, et al.,2015).

2.3.2.2.a p53 and its structure

p53 is a tumour suppressor protein and transcription factor that regulates cell cycle arrest, DNA repair and apoptosis. It is encoded by the tumour suppressor gene, TP53, a frequently mutated gene in human cancers (Brady, et al., 2010). This gene is located on the short arm of human chromosome 17 and comprises of 19,198 nucleotides with exon 1 to exon 11. The coding sequence of this gene begins at exon 2 and continues to exon 11 (Belyi, et al.,2010). p53 is often referred to as the guardian of the genome as it maintains genomic stability by initiating DNA repair and inhibiting DNA mutations (Read and Strachan, 1999).

The protein structure of p53 with 393 amino acids contains four domains: An N-terminal domain, core domain, oligomerisation domain (OD) and a C-terminal domain. The N-terminal (1-62 residues) has two transcriptional domains (TDA1 and TDA2). These domains play a major role in the tumour suppressor function of p53 (Brady, et al., 2010, Souza, et al., 2012). The N-terminal is followed by a proline-rich region (63-64 residues) and it is also important for p53 apoptotic activity. The DNA -binding domain is known as the p53 core domain and is located on residues 94-292. This domain contains several electropositive arginine amino acids and one zinc atom which binds to the DNA. The OD is localised at residues 326-356 and is responsible for tetramerisation, which is important for p53 activity (Kamaraj and Bogaerts, 2015). The C-terminal regulatory domain is found at 363-393 amino residues acts as a flexible region and it also plays role in the downregulation of central DNA binding domain (Tanaka, et al., 2018)

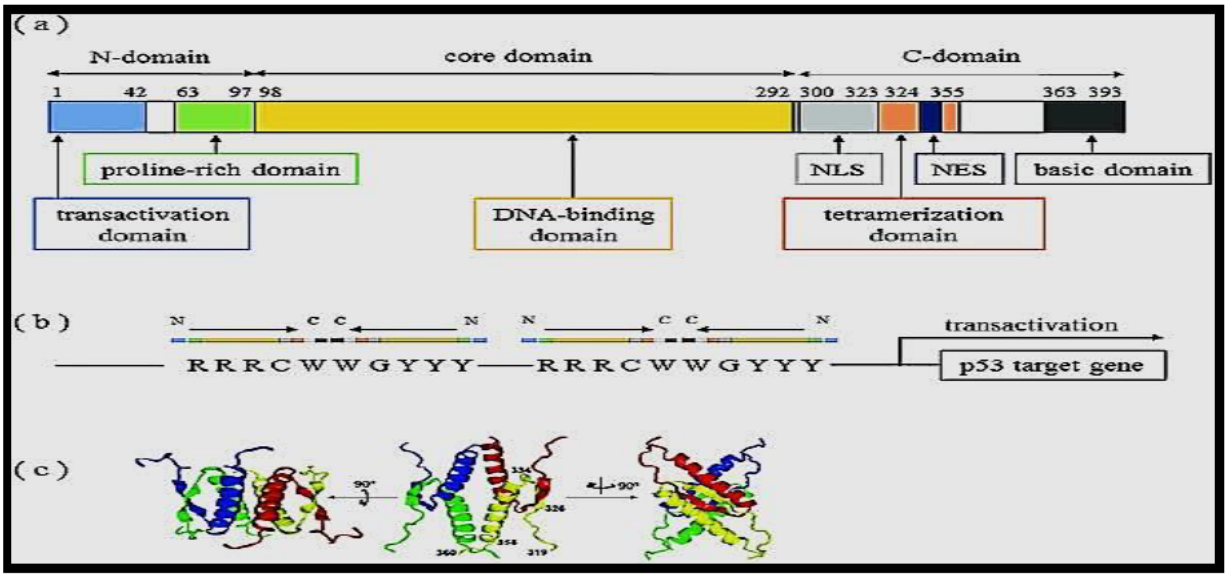

Fig 2.5: p53 structure (Tanaka, et al., 2018).

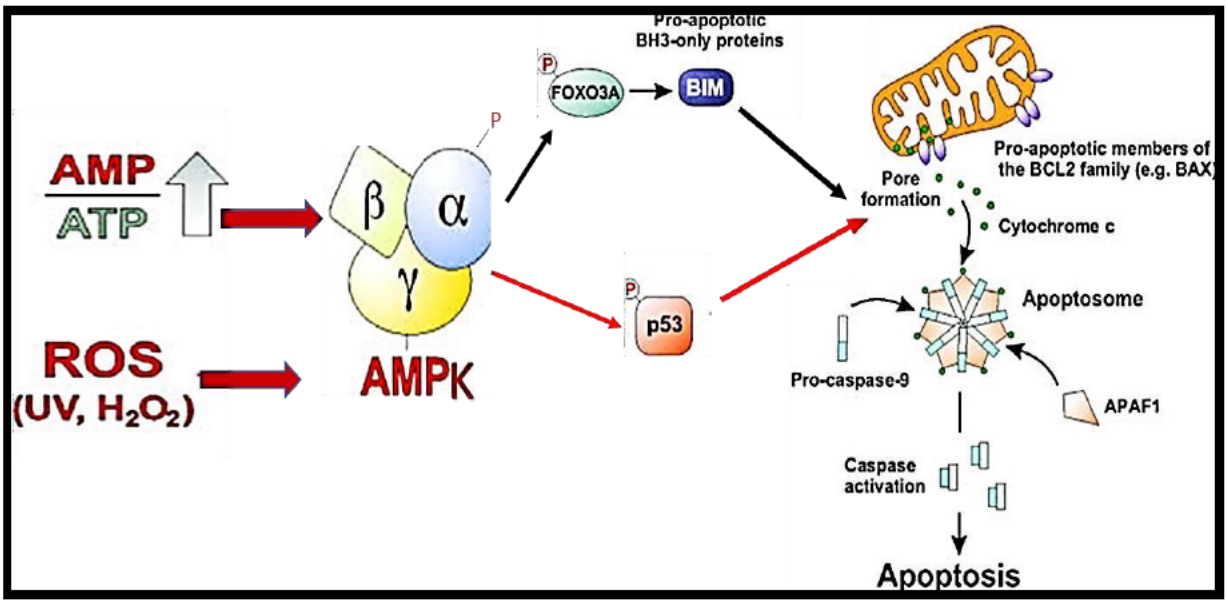

Fig 2.6: Apoptosis induced through AMPK signalling pathway (Carcadi, et al., 2012), (modified by the author).

2.4 Apoptosis

Apoptosis is a programmed cell death that is executed by caspases (Walsh, et al., 2008) and is required to help maintain an internal balance between cell death and renewal (Xu, et al., 2018). It serves as a natural barrier to inhibit tumourigenesis (Su, et al., 2015). The activation of caspases follows cell death stimuli (Walsh, et al., 2008) and results in structural

features of dying cells such as cell membrane blebbing, and formation of apoptotic bodies that are engulfed by phagocytes (Chen, et al., 2014).

Apoptosis can occur via two pathways; a death-receptor pathway (extrinsic) which is activated by death receptors on the cells surface or a mitochondrial pathway (intrinsic) which results in the release of cytochrome c from the mitochondria (Chen, et al., 2014). A study by Su et al., (2015) explained that there are other alternative apoptotic signalling pathways, and these include chronic endoplasmic reticulum (ER) stress which induces apoptosis through inositol-requiring protein-1 activity, however, these pathways may interact with the mitochondria and death receptor at some point. Various factors such as oxidative stress, DNA damage, tumour suppressors, (e.g., p53), mammary serine protease inhibitor, death-associated protein, and NF-κB contributes to apoptosis regulation (Su, et al., 2015).

2.4.1 Caspases

Caspases are essential mediators which help to accomplish the process of apoptosis (Yang, et al., 2016). They are members of the cysteine protease family with specific substrate cleaving function at the site after aspartic acid residues in the target amino acid sequences (Kominami, et al., 2012). Caspases exist in inactive forms in the cells, however, when they receive a death signal, caspases undergo dimerisation and cleavage, therefore changing into active forms (McIlwain, et al., 2012). Caspases involved in the apoptosis pathway are classified into two major classes, the executor, and the initiator caspases (Yang, et al., 2016). The initiator caspases include caspases 2, 8, 9 and 10, whereas the executors include 3, 6 and 7 (Walsh, et al, 2008).

2.4.1.1 Initiators of apoptosis

Initiator caspases are protein degrading enzymes with long pro-domains (approximately 90 amino acids). They are initially synthesised as monomeric pro-caspase. The pro-domains enable the initiator caspases to interact with specific signalling complexes. Caspase 8 pro-domains contain death effector domains, whereas prodomain of caspase 9 has a caspase recruitment domain/CARD (Malladi, et al., 2009). They are acknowledged for their role of activating their downstream target, the executor caspases. (McIlwain, et al., 2012). During the process of apoptosis, the initiator caspases couple the cell death stimuli to the executor (effector) caspases (Walsh, et al., 2008). The initiator caspases become active by self-cleaving, and this process is known as auto-activation (Kominami, et al., 2012). Pro-caspase is converted into an active form through cleaving activity which occurs in a demarcated

order, thus synthesising tetramer (2 small and 2 large subunits) of the fully developed protease (Chang, et al., 2003). In a study by Kruidering et al., (2000), it was suggested that pro-caspases can be activated via three mechanisms, namely, recruitment, auto-activation, and trans-activation. The study further explains that these mechanisms are used by all the initiator pro-caspases to transform into mature active forms of proteases.

2.4.1.2 Executor caspases complete apoptotic cell death

Executor caspases act on various apoptotic pathways to accomplish cell death (Su, et al., 2015). Unlike initiator caspase, executor caspases are originally synthesised as inactive dimers. They are synthesised as inactive dimers to prevent any inappropriate activation (McIlwain, et al., 2012). These dimers are activated through proteolytic cleavage at loops of their monomers. The structure of the executor caspases changes, therefore, resulting in an active form of effector caspases and this occurs subsequent to loop cleavage (McStay, et al., 2008). Upon activation, one executor caspase can initiate cleaving and activation of other effector caspases (McIlwain, et al., 2012). Activated executor caspases cleave a variety of intracellular substrates and will ultimately lead to apoptosis. The most studied and characterised executors are caspases 3 and 7 (Qu, et al., 2014).

2.4.1.2.a Caspase 3 and 7

Caspases 3 and 7 are key effector caspases required to execute apoptotic cell death. These executors have analogous protein structures, cleave similar substrates, and have the same apoptotic functions (Qu, et al., 2014). However, the two caspases contain different sequences at their N-terminal sites, and this includes N-peptides as well as 23-28 residue segments which are removed during zymogen activation (Denault, et al., 2003). Caspase 3 is activated by both crucial initiator caspases 8 and 9 through proteolytic cleavage, thus suggesting the importance of this enzyme in both mitochondrial and death receptor apoptosis (Seervi, et al., 2015). Caspase 7 is cleaved and activated by caspase 3 (Gafni, et al., 2009). Caspase 3 and 7 cleaves numerous structural and regulatory proteins which are required for cell maintenance and survival. Upon cleaving the substrates such as Poly (ADP-ribose) polymerase/PARP, the cells are degraded (Seervi, et al., 2015).

2.4.2 Extrinsic (death-receptor) pathway

An extrinsic pathway is triggered by the activation of death receptors on the surface of the cell membrane. This occurs through binding of ligands such as TNF, TNF-related apoptosis-

inducing ligand (TRAIL) or FasL (Chen, et al. 2014). These death ligands interact with their cognate receptors to transmit extracellular information into the cytoplasm through the cytoplasm adaptor molecules (Salvesen, et al., 2014). Until recently, only six death receptors have been described in mammals, and they include TNFR1, Fas, DR3, DR4, DR5, and DR6 (Kominami, et al., 2012). Signalling through TNRF1 and DR3 is associated with proinflammatory, whereas others induce cell death (Danial, et al., 2018). TNRF1 and Fas are the most studied death receptors, FasL binds to the Fas receptor, whereas TNF and lymphotoxins α binds to the TNRF1 receptor (Courageot, et al., 2003). DR4 and DR5 are death receptors for TRAIL (Gibson,2004).

Death receptors are members of tumour necrosis factor receptor gene superfamily (Courageot, et al., 2003). Stimulation of the receptors is followed by death domains (receptor's intracellular domains) binding to the adapter protein Fas-associated death domain (FADD). This results in the formation of a complex called death-inducing signalling complex (DISC) and assembly of pro-caspase 8 (Chen, et al., 2014). Subsequently, autoactivation of caspase 8, and initiation of a caspase cascade (Danial, et al., 2018).

2.4.3 Intrinsic (mitochondrial) apoptotic pathway

The intrinsic pathway is induced by intracellular stimuli such as DNA damage and cellular stress including oxidative stress, cytotoxic drug treatment, etc (Kominami, et al., 2012). It involves the formation of a complex called apoptosome (Su, et al., 2015). Apoptosome complex consists of pro-caspase 9, apoptotic protease activating factor 1 (Apaf-1), and cytochrome c (Su, et al., 2015). Activation of caspase 9 leads to the commencement of caspase cascade, thus resulting in the stimulation of caspase 3, 7 and/ or 6 (Kominami, et al., 2012). Apaf-1 in the cytoplasm exists as an inactive monomer. However, when cells experience stress, they release cytochrome c (Cyt C) from the mitochondria. Subsequent to its release, Cyt C will bind to the WD domain of the Apaf-1 monomer and thus resulting in structural change which will expose the nucleotide-binding site in the nucleotide-binding and oligomerisation domain of Apaf-1. Apaf-1 undergoes a secondary structural change when deoxy-ATP binds to the nucleotide-binding site thus exposing oligomerisation and CARD domains of activated Apaf-1 monomer. Approximately seven activated Apaf-1 forms an oligomeric complex with a centre containing CARD motif which plays a crucial role in recruiting and activating caspase 9 (McIlwain, et al., 2012).

2.5 Liver is a primary filtration system in human body.

The liver is the second largest organ in the body involved in biotransformation, detoxification, protein production, etc. It is located between the gastrointestinal tract (GIT) organs and the heart (Ramadori, et al.,2008). The liver has dual inputs for blood supply. Approximately 80% of its blood is supplied through a portal vein from the gut whereas 20% is provided by the hepatic artery from vascularization. The blood from the gut is accumulated by bacterial products, environmental toxins, and food antigens, therefore the liver filters the blood before supplying the rest of the body (Gao, et al., 2008). Liver is the main organ that metabolise and eventually excretes the exogenous chemical. Consequently, the liver cells are exposed to high quantities of these xenobiotics, and this can cause liver dysfunction, cell damage and even liver failure (Jaeschke, 2008).

2.6 HepG2 cells

The HepG2 cell line is a liver cell line that was derived from a 15-year-old male of European ancestry (Zhou, et al.,2019). HepG2 cells refer to liver cells that can grow and proliferate at a high rate. They are epithelial in morphology and have retained various liver enzymes involved in biotransformation and detoxification. HepG2 cells have physiologic functions and properties similar to that of typical liver cells/hepatocytes and are thus widely used in biomedical research to assess hepatotoxicity and drug metabolism (Donato, et al., 2014).

CHAPTER 3: MATERIAL AND METHODS

3.1 Materials

The HepG2 cells were purchased from Highveld Biologicals (Johannesburg, South Africa). FA (F6513, Sigma Aldrich) and FB_1 (62580, Cayman chemical) were acquired from Sigma-Aldrich (St. Louis, MO, USA). Cell culture equipment such as 25 cm^3 culture flask, etc. and reagents (Eagle's Minimum Essentials Medium, etc.) were procured from Lonza Biotechnology (Basel, Switzerland). Luminometry reagents were obtained from Promega (Madison, USA). Real-time PCR (qPCR) primers were synthesised by Inqaba Biotech (South Africa). Western blots reagents were obtained from Bio-Rad (Hercules, CA, USA). All other reagents were purchased from Merck (Darmstadt, Germany).

3.2 Cell culture

3.2.1 Introduction

Cell culture refers to an *in vitro* process where cells of interest are allowed to grow in a controlled environment. These cells are kept in a controlled environment subsequent to their isolation from the living tissue (Carter, et al., 2015). In this study, HepG2 cell lineage was used. HepG2 cells are a human cancer cell line derived from the liver tissue of a 15-year-old male of Caucasian ancestry who was diagnosed with hepatocellular carcinoma. The cells are adherent and epithelial in morphology that grow as a monolayer in small aggregate. HepG2 cells contain 55 chromosome pairs and have similar physiological functions to normal human hepatocytes. They are known for their high proliferation capacities and are reliable models for hepatotoxicity studies due to first pass metabolism and their ability to detoxify a wide range of xenobiotics (Mersch-Sundermann, et al., 2004).

3.2.2 Cell culture conditions

HepG2 cells were cultured in 25cm^3 sterile cell culture flasks with complete culture media (CCM; Eagle's Minimum Essentials Medium (EMEM) containing 10% foetal calf serum, 1% penicillin-streptomycin-fungizone and 1% L-glutamine) at 37◦C with 5% CO_2 humidified incubator. CCM was replenished every two days until approximately 90% confluency was

obtained. Thereafter, the cells were incubated with FA and FB_1 for a period of 24 hrs. An untreated control (CCM only) was also prepared.

3.3 Treatment preparations

A stock solution of FA (10mg/ml) and FB_1 (5mM) was prepared in 0.1 M phosphate buffered saline (PBS). HepG2 cells were then simultaneously incubated (37°C, 5% CO_2, 24 hrs) with a range (5µM, 27µM, 100µM, and a combination of the individual FA (104 µg/ml) and FB_1 (200µM) IC_{50}s) of FA and FB_1.

3.4 MTT (3-(4,5-dimethylthiazol-2-yl)-2,5-diphenyltetrazolium bromide) assay

3.4.1 Principle

MTT assay is the most commonly used colorimetric quantitative assay to determine cytotoxicity/cell viability (Aslantürk, 2018). It uses a 3-(4,5-dimethylthiazol-2-yl)-2,5-diphenyltetrazolium bromide or methylthiazol tetrazolium (MTT) that cleaved and converted into insoluble purple formazan crystals through activities of a mitochondrial enzyme called succinate dehydrogenase. This reaction only takes place in live metabolically active cells as dehydrogenase enzymes are inactivated in dead cells and the reaction is dependent on the synthesis of NADH. The resultant formazan product is solubilised with Dimethyl sulfoxide (DMSO), dimethylformamide, or SDS (Riss, et al., 2016) and can be measured using a spectrophotometer at a wavelength of 570nm. The intensity of the purple formazan produced is directly proportional to the number of viable cells.

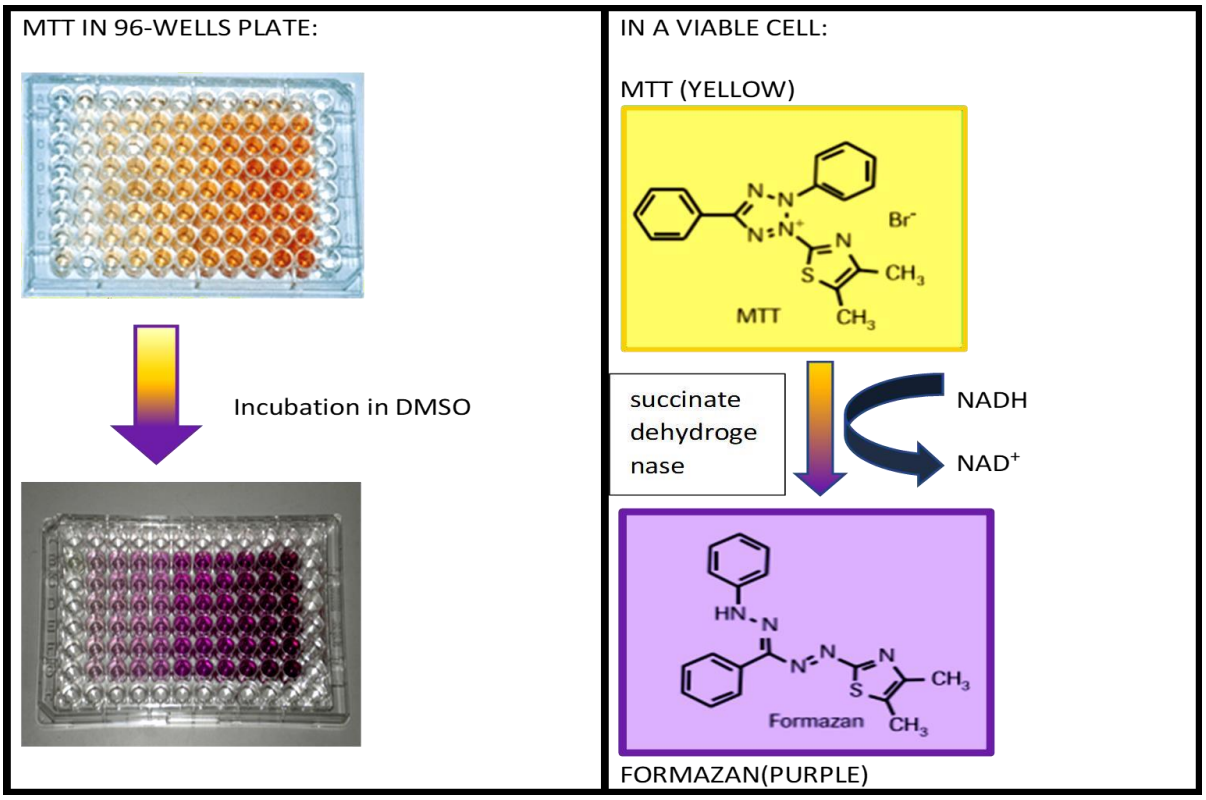

Fig 3.1: Principle of the MTT assay. Reduction of yellow MTT dye into measurable purple Formazan by mitochondrial succinate dehydrogenase (Prepared by the author).

3.4.2 Protocol

HepG2 cells were detached by trypsinisation and seeded (20,000 cells/well) in a 96-well microtiter plate. The plate was then incubated (37°C) in the humidified incubator overnight to allow the cells to adhere. Following overnight incubation, the cells were rinsed 3 times with PBS and co-treated with concentration ranges (0.25, 5, 25, and 50mM) of FA and FB_1 in triplicate. The plate was incubated for 24 hrs at 37°C in a humidified incubator. Thereafter, the treatments were removed and MTT salt (5mg/ml, 20µl) and CCM (100µl) were added to the wells and incubated for 4 hrs. Subsequently, 100µl DMSO was added to the wells followed by 1 hr incubation. The absorbance was measured using a spectrophotometer at 570nm and a reference wavelength of 690nm. The results were expressed as percentage cell viability vs. concentration of FA and FB_1 co-treatment. The absorbances were used to construct a survival curve from which the IC_{50} was determined. In addition to the IC_{50} (27µM), 4 different concentrations (0µM/control, 5µM, 100µM and combined IC_{50}s (104µg/ml FA and 200µM FB_1) were selected and used for all subsequent assays.

3.5 Luminometry assay (ATP and Caspases assay)

3.5.1 ATP assay Principle

Luminometry is a laboratory technique used to assess cellular ATP and/ caspase activities (Marroquin, et al, 2007). Adenosine triphosphate (ATP) is a crucial chemical energy reservoir in metabolically active cells that is required to carry out cellular processes, such as apoptosis. ATP molecules are essential for the function of Apaf-1 which establishes the activation of caspases (Ferarri, et al., 1998). Living cells produce ATP through glycolysis and oxidative metabolism and this reflects their viability (Paris, et al., 2015). ATP assay is a luminometric assay required to determine cell viability based on quantification of the ATP present which signals the presence of living cells (Riss, et al., 2016). The principle of this assay involves the emission of light by luciferin and oxygen-dependent enzyme luciferase (Casem, 2016). However, for this reaction to occur, other co-factors for luciferase such as Mg2+ ions and ATP are required. In the presence of its co-factors and substrate, luciferase can generate light. The light produced is directly proportional to the level of ATP (Hastings and Johnson, 2007).

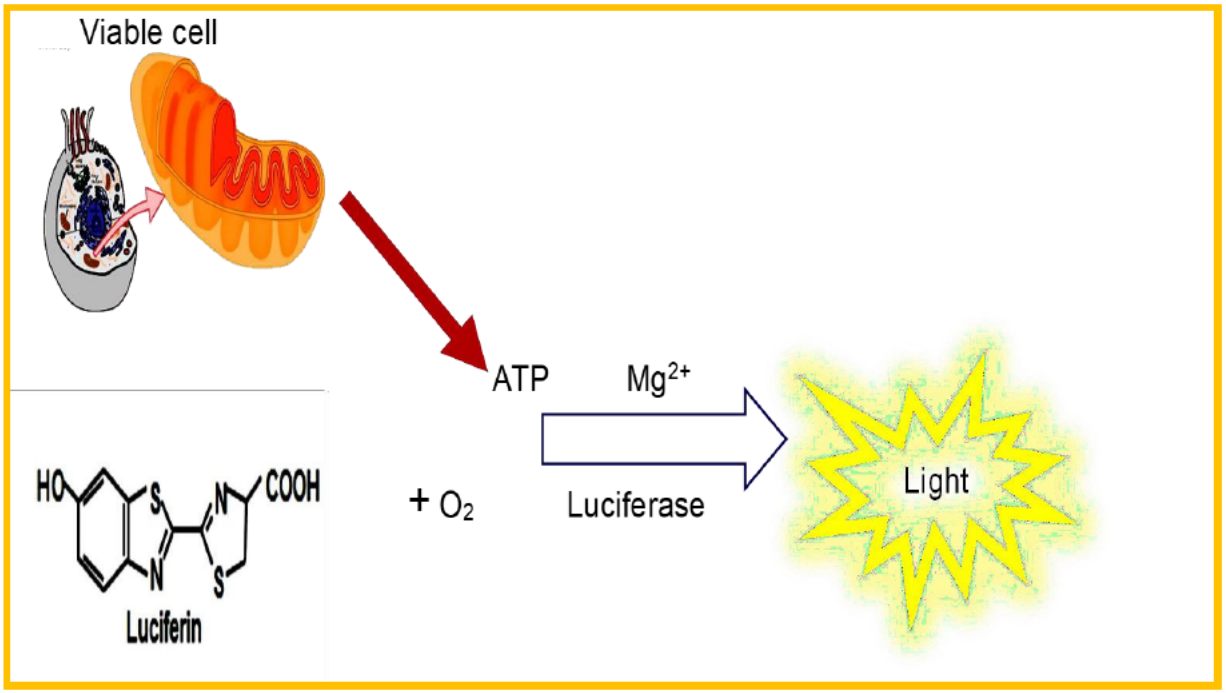

Fig 3.2: Principle of ATP assay. Production of light by luciferin and oxygen-dependent luciferase in the presence of ATP and Mg ions (Prepared by the author).

3.5.2 Caspase assay principle

Caspases are proteases that initiate and execute apoptosis (McStay and Green, 2014). They are produced in an inactive form and become activated after receiving a signal induced by either physiological or pathological stimuli (Kaufmann, et al.,2007). Upon activation, caspases cleave their respective substrates at the carboxy-terminal peptide bond of the aspartic acid residue (McStay and Green, 2014). Activation of these proteases can be detected by measurement of their activity (Kaufmann, et al., 2007).

Caspase assay is based on the cleavage and detection of a bioluminescent substrate. The substrates are labelled with a specific sequence at the C-terminal (O'brien, et al., 2003). The sequences are specific to each one of the caspases and this includes; DEVD for caspase-3 and -7, LEHD for caspase-9, and IETD for caspase-8 (Pop, et al., 2008). Subsequent to cleavage of the substrate, a free amino-luciferin will be released and react with an oxygen-dependent enzyme called luciferase, therefore, producing a luminescent signal/measurable light. The signal produced can then be captured by a luminometer (O'brien, et al., 2003). The quantity of the signal generated is directly proportional to caspase activity.

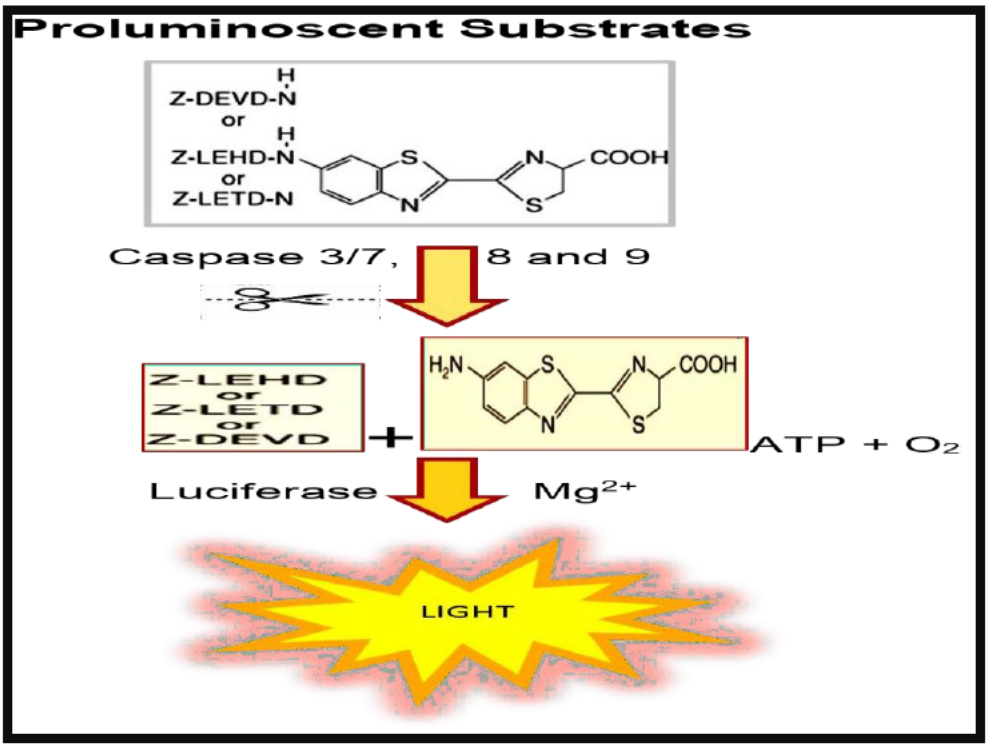

Fig 3.3: Principle of the caspase assay. Caspase 3/7, 8 and 9 cleaves the substrates, therefore releasing amino-free luciferin which then reacts with Luciferase to emit light (prepared by the author).

3.5.3 Luminometry protocol

Following treatment with FA and FB_1 for 24 hrs, HepG2 cells were trypsinised and seeded (20,000 cells/well) into an opaque 96-well microtiter plate in four replicates. Thereafter, 20µl of the ATP-Glo and Caspase-Glo reagents (see table 3.1) were added to each well and the plate was incubated at room temperature for 30 min in the dark. The luminescent signal was then measured using a Modulus™ microplate luminometer and the results were expressed as mean relative light units.

Table 3.1 Name and catalogue number for caspases and ATP kit

Reagent kit name	Catalogue number and company name
Caspase-Glo-9	G8210, (Promega, Madison, USA)
Caspase-Glo-8	G8200, (Promega, Madison, USA)
Caspase-Glo-3/7	G8090, (Promega, Madison, USA)
ATP (cell-titer-Glo ATP Assay)	G7570, (Promega, Madison, USA)

3.6 Thiobarbituric Acid Reactive Substance (TBARS) assay

3.6.1 Principle

The TBARS assay is a common spectrophotometric method used to determine malondialdehyde (MDA) which is a by-product of lipid peroxidation (Hodge, et al.,1999). TBARS assay is based on the production of coloured end-product (1:2 adduct/MDA-TBA adduct) when MDA reacts with thiobarbituric acid /TBA in the presence of heat and acid. This product can absorb light at 532-535nm (Schaich, 2016). The synthesis of MDA-TBA occurs through nucleophilic attack which involves TBA carbon-5 and MDA carbon-1. This is followed by dehydration and a similar reaction with the second TBA molecule, thus producing a pink-red colour. A spectrophotometer is then used to measure the intensity of the pigment formed from a concentration of MDA-TBA. The intensity measured is an indicator of lipid peroxidation. Lipid peroxidation is the oxidative degradation of lipids by ROS; therefore, lipid peroxidation indicates an increase or presence of ROS during the process of oxidative stress. TBARS such as MDA increases in response to oxidative stress and are produced as a by-product of lipid peroxidation (Grotto, et al., 2009).

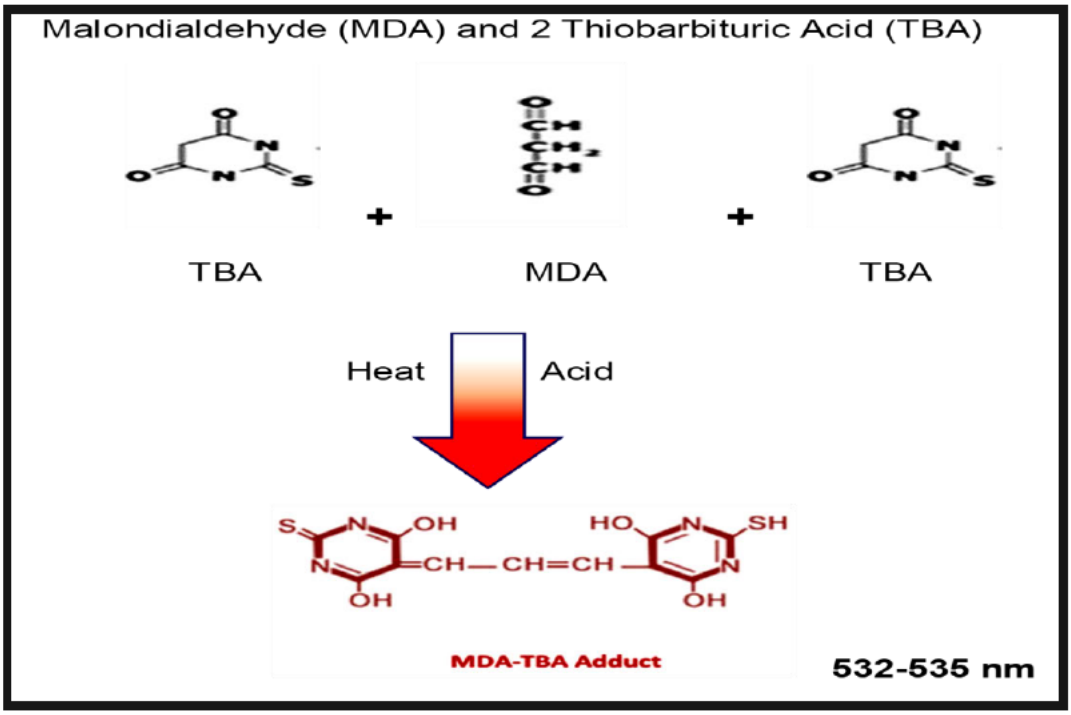

Fig 3.4: Principle of the TBARS assay. Production of MDA-TBA adduct from the reaction of MDA and 2 TBA (Prepared by the author).

3.6.2 Protocol

Supernatants from control as well as FA and FB_1 co-treated HepG2 cells were removed and used to conduct the TBARS assay. Supernatants (400µl) from the control and treated cells as well as 7% H_3PO_4 (200µl) and TBA/BHT solution (200µl) were added to test tubes. The positive control consisting of 200µl of 7% H_3PO_4, TBA/BHT solution (200µl) and 1ul MDA; and negative control containing 7% H_3PO_4 (200µl), 3mM HCl (400µl) was prepared. Thereafter,200µl of 1mM HCl was added to all samples to bring the pH to 1.5. Samples were boiled at 100°C for 15 min in a water bath. The test tubes were allowed to cool at room temperature and butanol (1ml) was added to the samples causing the samples to separate into 2 distinct phases. The upper butanol phase (500µl) was transferred into fresh 1.5ml micro-centrifuge tubes and centrifuged (13,200 rmp, 6 min, 24°C). The supernatants (100µl) were then plated in triplicate in a 96-well microtiter plate and OD was measured at a wavelength of 532nm (reference wavelength: 600nm).

3.7 RNA isolation protocol

To isolate total RNA, the supernatants were discarded, and the cells washed three times with 0.1M PBS. Thereafter, Qiazol (500µl) and PBS (500µl) were added to each flask and

the flasks were incubated for 5 min at room temperature. Following incubation, cells were lysed using a cell scraper. The Qiazol containing cells was transferred into appropriately labelled micro-centrifuge tubes and stored overnight at -80°C.

After overnight storage, 100µl chloroform was added to the thawed samples and centrifuged for 15 min at 12,000xg, 4°C. The aqueous phase containing the crude RNA was transferred into fresh 1.5ml micro-centrifuge tubes, and 250µl isopropanol was added to precipitate the RNA. The samples were stored overnight at -80°C.

Thawed samples were centrifuged (12,000xg, 20min, 4°C), the supernatant was discarded, and the pellet was washed with 500µl of 75% cold ethanol. Thereafter, samples were centrifuged (7,400xg, 15min, 4°C) and the pellet was air-dried for 30 min. The RNA pellet was re-suspended in nuclease-free water (15µl) and quantified using the Nanodrop2000 spectrophotometer (Thermofisher Scientific). The A260/A280 ratio was used to assess the RNA purity. The concentration of RNA was standardised to 1,000ng/µl and used to prepare complementary DNA (cDNA).

3.8 cDNA Synthesis protocol

The standardised RNA samples and maxima H minus cDNA kit (K1652, Thermofischer Scientific) was used to synthesise cDNA. A 15µl reaction mix containing 0.25µl oligo $(dT)_{18}$ primer, 1µl of 10mM dNTP mix, 12,75µl nuclease-free water, and 1µl RNA sample was prepared and incubated in a thermocycler (GeneAmp® PCR System 9700, Applied Biosciences) at 65°C for 5 min. Thereafter, a 4µl of RT buffer and 1µl Maxima RT enzyme mix was added to each sample and incubated as follows: 5min at 25°C, 30min at 42°C and 5min at 85°C.

3.9 Real-time PCR (qPCR)

3.9.1 Principle

Real-time quantitative polymerase chain reaction (qPCR) refers to a chain reaction-based laboratory technique with the ability to measure/detect the amplified target nucleic acids (PCR amplicons) during each cycle of PCR while the reaction is still in exponential phase (Pestana, et al., 2009). The principle is based on the ability of Taq polymerase to generate a complementary strand using the offered DNA template. During the process, double-stranded DNA sequences are amplified exponentially when all the reagents are fresh and available

(Rao, et al, 2013). The qPCR allows precise quantification of RNA and DNA with greater reproducibility. PCR allows the production of specific DNA fragments. It requires 6 components and needs to be performed at certain conditions to synthesis the amplicons (Kubista, et al., 2006).

3.9.1.1. Components of PCR

a. Template DNA that contains the target sequence to be amplified which ranges between 100-1000 base pairs in length.
b. Primers (Reverse and forward) refers to small fragments of DNA that are complementary to the 3'ends of each DNA template. The primers bind to the DNA template at 3' ends, therefore an enzyme known as Taq polymerase will bind to these primers so that elongation can occur.
c. Taq polymerase- polymerise new DNA strands. This enzyme is heat stable and can remain intact during the denaturation step of the PCR. It is originally isolated from a thermophilic bacterium known as *Thermus aquaticus*. It elongates the new strand from free nucleotides by using single-stranded DNA as the DNA template and primers to initiate DNA synthesis.
d. Deoxynucleotide triphosphates (dNTPs) are the building blocks that Taq polymerase uses to synthesise a new strand of DNA. These building blocks consist of four nitrogenous bases, namely, adenine, thymine, cytosine, and guanine.
e. Buffer - It provides a suitable chemical environment for optimum activity and stability of Taq polymerase.
f. Divalent Cation (Magnesium ion, Mg^{2+}) is the most commonly used cation during the PCR technique. Magnesium ions for PCR are usually found in the buffer. It acts as the cofactor for Taq polymerase and is essential catalyser in PCR. Adequate Mg^{2+} concentrations are important for controlling the specificity of the reaction; a low Mg^{2+} concentration requires more stringent base pairing in the annealing step. Insufficient Mg^{2+} concentration in a PCR mixture can result in low yield of PCR products and can also cause the failure of the reaction, whereas, excess Mg^{2+} ions increase the yield of non-specific products by causing the fidelity of Taq polymerases to be reduced and it also promotes misincorporation.

3.9.1.2. Conditions and steps of PCR

There are 3 crucial steps carried out during PCR and each has a specific temperature at which they are performed. These steps are usually repeated for 25-40 times to allow sufficient amplification;

a. Denaturation

Double-stranded DNA is denatured or separated into two single-stranded DNA molecules by breaking the hydrogen bonds between complementary base pairs. Denaturation is usually performed at a temperature between 94-97°C and for 20-30 sec.

b. Annealing

In this step, primers (reverse and forward) bind to the complementary DNA sequence of the single-stranded DNA template. Annealing requires the temperature to be lowered to approximately 50-65°C and takes place for about 20-40 sec.

c. Elongation.

In this step, Taq polymerase binds to the primer and uses dNTPs to extend/elongate the new strand that is complementary to the single-stranded DNA template. Elongation occurs at 72° C for approximately 30 sec.

There are many methods used to analyse data from qPCR and these include; threshold cycle (CT), standard curve, etc. These methods involve the removal of background fluorescence or the amount of fluorescence measured before any detectable amplicons start. The background fluorescence may be the results of unbound fluorochrome, for example; SYBR Green I or fluorochrome bound to double-stranded cDNA and annealing of the primer to nontarget DNA sequences (Rao, et al., 2013). The CT method refers to the fractional cycle number at which a certain amount of DNA is reached. The CT method of quantitation reported as fold change ($2^{-\Delta\Delta Ct}$) and adapted from Livak and Schmittgen, involves analysing gene expression by comparing the target gene with the house-keeping gene (Rao, et al., 2013).

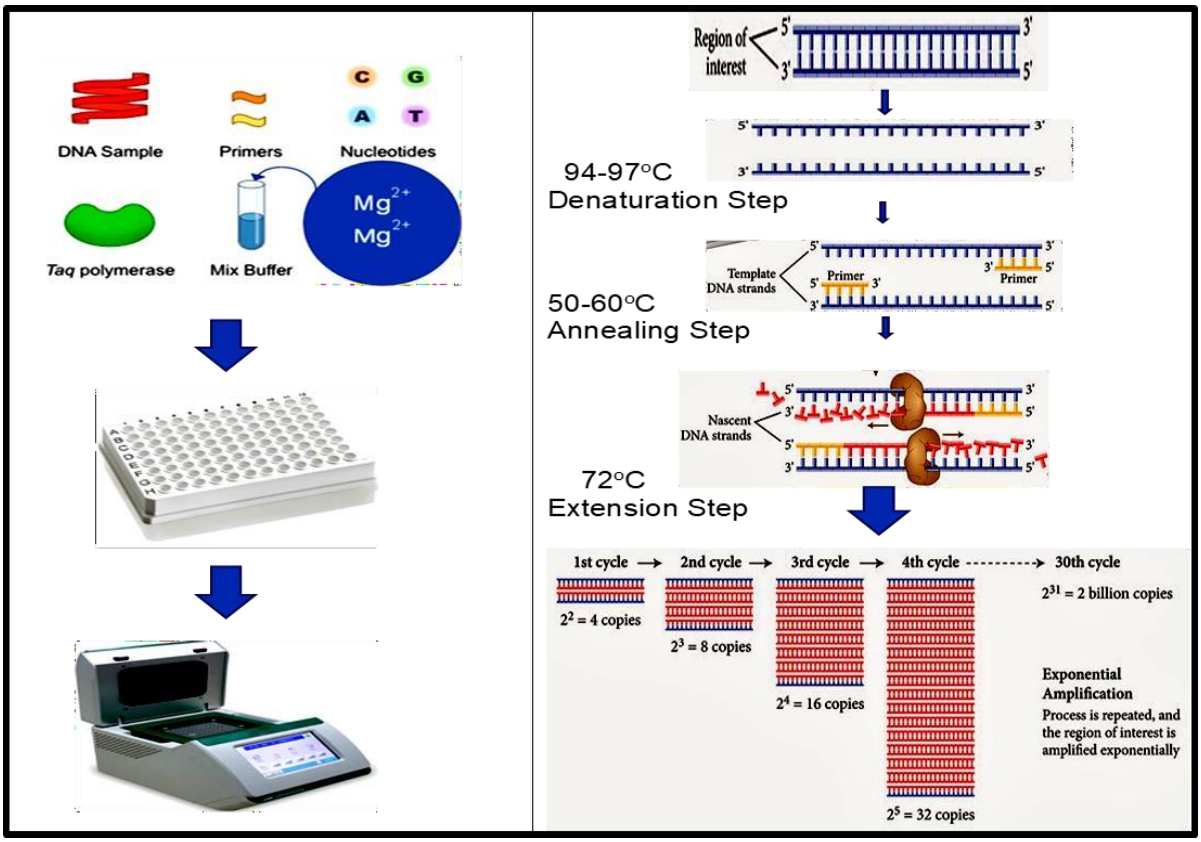

Fig 3.5: Principle of qPCR. Taq polymerase binds to the primers to synthesise new DNA strands using a reference DNA template and dNTPs in the presence of magnesium ions (prepared by author).

3.9.2 Protocol

The Powerup SYBR™ Green Master Mix (A25742) was used to analyse gene expression according to the manufacturer's instructions. FOXO3a mRNA expressions were investigated using the specific forward and reverse primers (see table 3.2). Glyceraldehyde-3-phosphate dehydrogenase (GAPDH) was used as the housekeeping gene. The reaction mixture consisted of SYBR green (5µl), forward primer (25µM, 1µl), reverse primer (25µM, 1µl), nuclease-free water (2µl), and cDNA template (1µl). All reactions were carried out in triplicate.

All the samples were amplified using the CFX96 Touch™ Real-Time PCR Detection System (Bio-Rad). The PCR was initiated with the following thermocycler profile: The initial denaturation for 8 min at 95°C, followed by 40 cycles of denaturation (95°C, 15 sec); annealing (40 sec; 57.8°C) and extension (72°C, 30 sec).

Table 3.2 Sequences of FOXO3a and GAPDH primers (prepared by author)

Gene	Forward primer sequence	Reverse primer sequence
FOXO3a	5'-CTTGAAGGATAAGGGCGACAG-3'	5'-TCGTCCTGGACTTCATCCAAC-3'
GAPDH	5'-TCCACCACCCTGTTGCTGTA-3'	5'-ACCACAGTCCATGCCATCAC-3'

3.10 Protein isolation, quantification, and standardisation

Following treatment, the supernatants were removed, and the cells were rinsed three times in 0.1M PBS. Thereafter, 200µl cytobuster reagent containing protease inhibitors (Roche, catalogue no. 05892791001) and phosphatase inhibitors (Roche, catalogue no. 04906837001) was added to the cells, and the flasks were incubated on ice for 30 min. The cells were then mechanically lysed using a cell scraper, transferred to 1.5ml micro-centrifuge tubes, and centrifuged (10,000xg, 10 min, 4°C). The supernatants containing the crude protein extract was aspirated into fresh 1.5ml micro-centrifuge tubes until further quantification and standardisation.

To quantify and standardise proteins, bovine serum albumin (BSA) standards (0, 0.2, 0.4, 0.6, 0.8 and 1mg/ml) were prepared in distilled water. A 25µl of standard solutions were plated in triplicate and protein samples in duplicate in a 96-well microtiter plate. A working solution (200µl) consisting of 198µl BCA and 4µl CuSO4 was added to each well and the plate was incubated at 37°C for 30 min. The absorbance at 562nm was measured using a spectrophotometer (Bio-Tek µQuant Plate Reader). The absorbances of the BSA standards were used to construct a standard curve from which the concentrations of proteins were determined. The proteins were standardised to a concentration of 1.0mg/ml.

3.11 Western blot

3.11.1 Principle

Western blot is a molecular technique used to identify specific proteins from a homogenous mixture of different proteins. It is based on the principle of antigen-antibody binding where SDS-polyacrylamide gel is used to separate proteins according to their molecular weight. The western blot assay can be accomplished through 6 steps namely; sample preparation,

gel electrophoresis, proteins transfer, blocking, antibody incubation, and protein detection and visualisation.

3.12.1.1 Sample preparation

Before separation by sodium dodecyl sulphate polyacrylamide gel electrophoresis (SDS-PAGE), the protein samples are prepared in 1x laemmli buffer and incubated at 100°C in a water bath for 5 min. The laemmli buffer contains very crucial components (see table 3.3) with certain functions that allow for optimum SDS-PAGE.

Table 3.3 Components of Laemmli buffer and functions (prepared by author)

Components	Functions
Glycerol	It is required to add weight to the samples allowing the samples to sink easily into the wells of the gel in SDS-PAGE
SDS	Denatures proteins and imparts an overall negative charge enabling separation of proteins according to size.
β-mercaptoethanol	Acts as a reducing agent to break disulphide bonds and denature the proteins.
Bromophenol blue	Permits visualisation of the samples as they migrate through the SDS-gel.
Tris–HCl	Serves as the buffer and maintains pH.

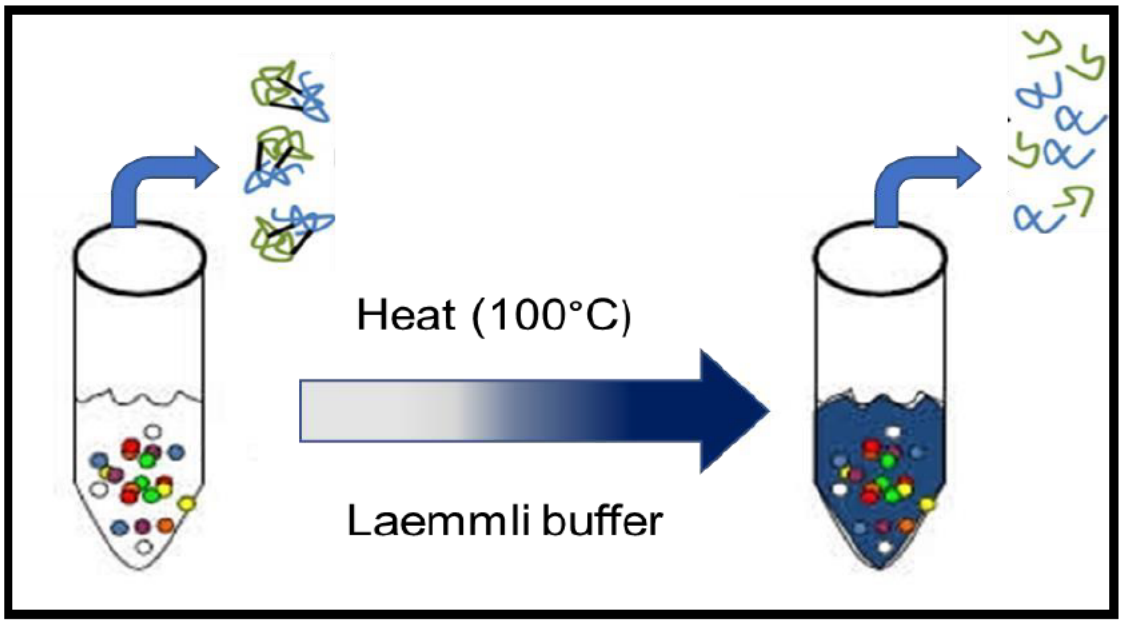

Fig 3.6: Preparation of samples for western blot. Components of Laemmli buffer denatures proteins and converts protein sample into violet to allow visualisation (Prepared by the author).

3.12.1.2 SDS-PAGE

An SDS-polyacrylamide gel is the most commonly used gel in western blot. The percentage of the gel that can be used is 5, 8, 10, 12 or 15%, however, this depends on the size of the target proteins. The smaller the weight of the protein of interest, the higher the percentage of the gels to be used. Two types of gels are used in western blot; resolving and stacking gel. The stacking gel contains the wells for sample loading and is required to pack all the proteins in a thin single band, and it is always at the top of the resolving gel, whereas the resolving/separating gel is needed to separate the proteins according to their size. Smaller proteins migrate faster compared to the large proteins and are usually found at the bottom of the gel whereas the larger proteins are found towards the top of the gel.

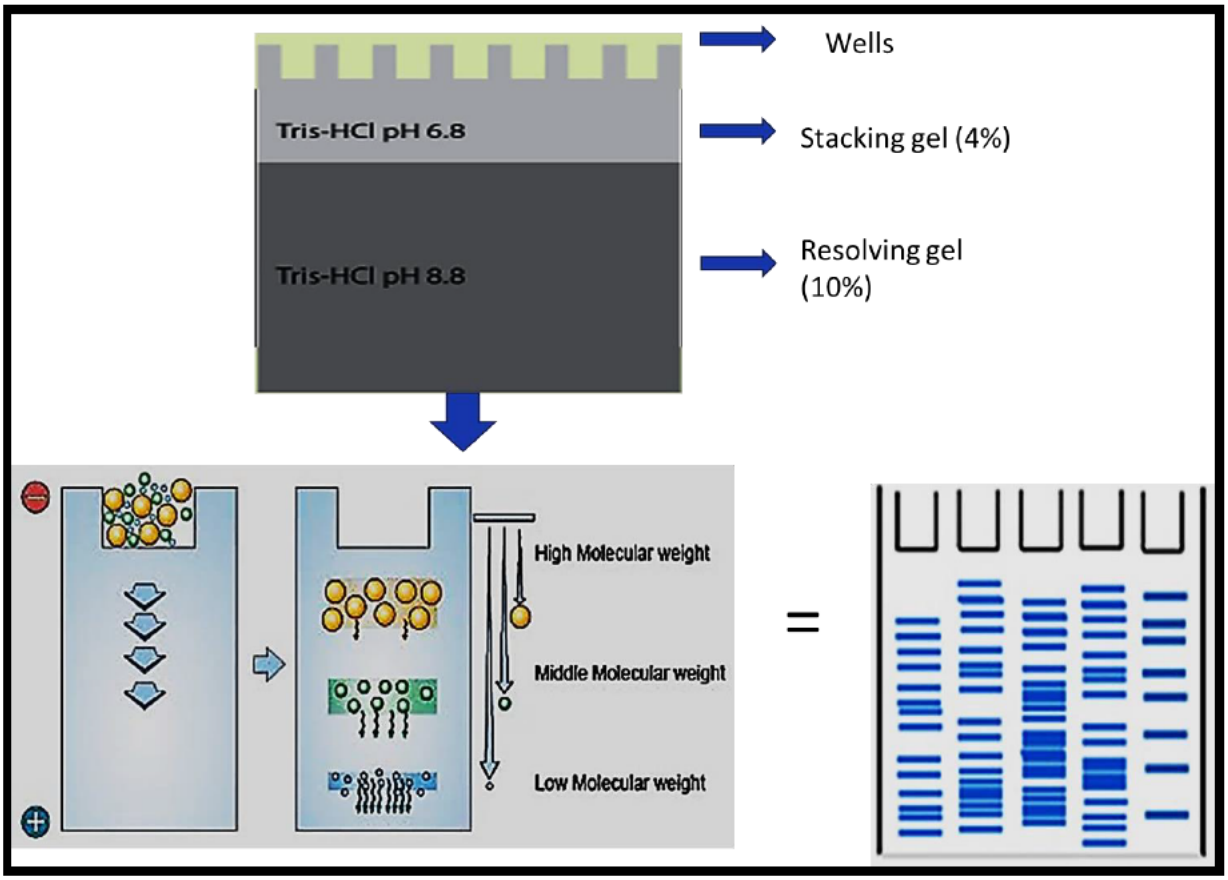

Fig 3.7: Migration of denatured proteins according to molecular weight (prepared by the author).

3.12.1.3 Protein transfer

The separated proteins are transferred from within the gel onto the membrane (e.g. nitrocellulose or polyvinylidene difluoride) to allow easy accessibility for protein detection. The membrane can absorb the proteins without altering their biological activities. The method used to transfer is referred to as electro-blotting which involves the use of perpendicular electric field to pull the proteins from the gel onto the membrane. A transfer sandwich composed of a fiber pad, membrane, gel and another soaked fiber pad.

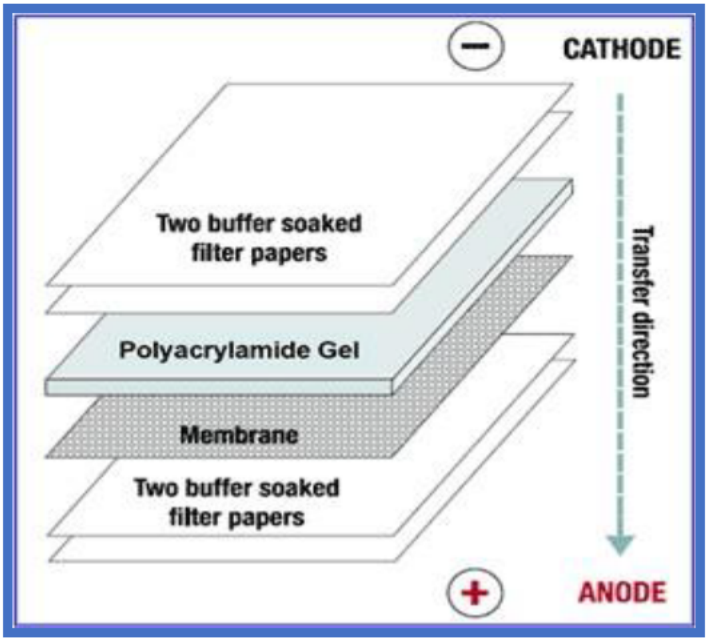

Fig 3.8: Transfer of proteins from the polyacrylamide gel to the nitrocellulose/ polyvinylidene difluoride membrane (Temmerman, et al., 2003).

3.12.1.4 Blocking

The membrane is incubated in blocking buffer containing 5% BSA in Tris buffered saline with 0.01% tween 20 to block the hydrophobic binding sites of the membrane. This will inhibit the antibodies from binding to the membrane non-specifically.

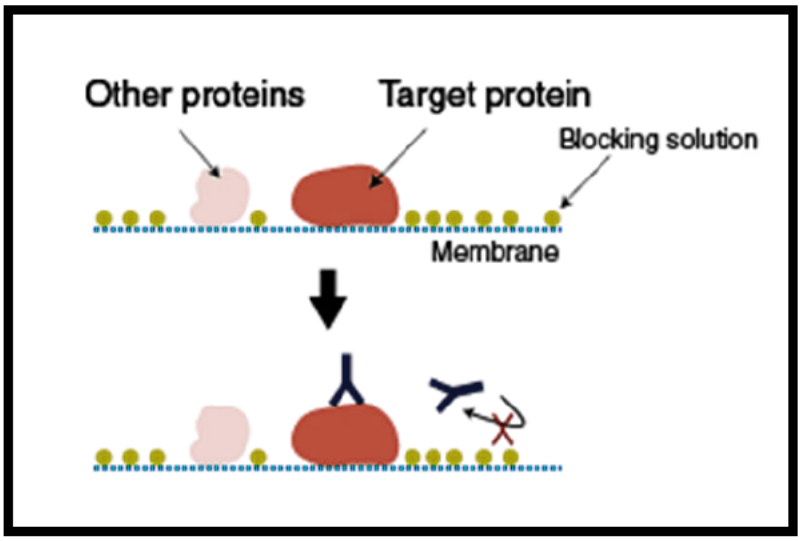

Fig 3.9: Blocking solution inhibits non-specific binding of antibodies by blocking the hydrophobic binding sites of the membrane (Yamada, et al., 2007).

3.12.1.5 Antibody incubation

Subsequent to blocking, the membrane is probed with primary antibodies that are specific to the protein of interest. Unbound primary antibodies are washed and removed from the membrane. After a wash with an antibody-buffer solution, the primary antibody-treated membrane is exposed to labelled/ specific enzyme-conjugated secondary antibodies which bind to the species-specific site of the primary antibody thus forming an antibody complex.

3.12.1.6 Protein detection and visualisation

Binding of secondary antibodies enhances signals, therefore allowing the detection of proteins. A substrate reacts with the enzyme on the secondary antibody, therefore, producing a coloured substance. This helps to identify densitometry and the location of the protein of interest. The size of the proteins is determined by comparing the protein bands to the molecular weight marker. The electrochemiluminescence (ECL) detection system is used for detection.

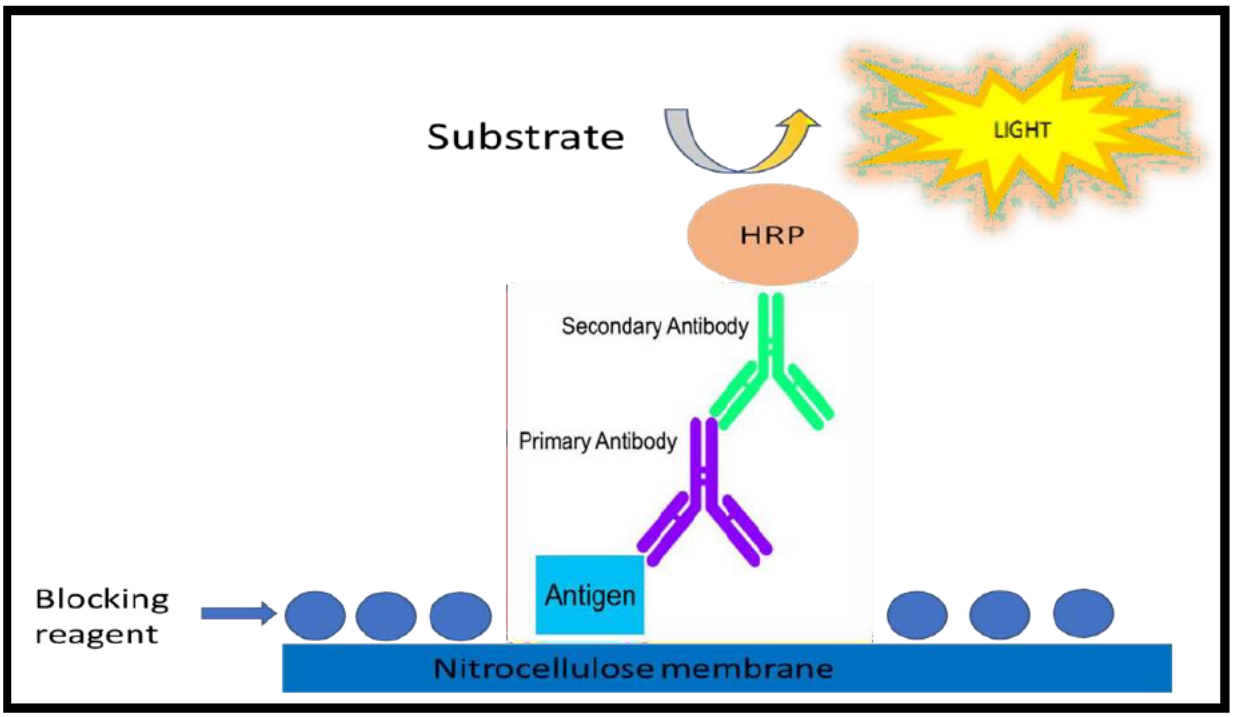

Fig 3.10: Emission and detection of light released when a substrate reacts with the enzyme on the secondary antibody (prepared by the author).

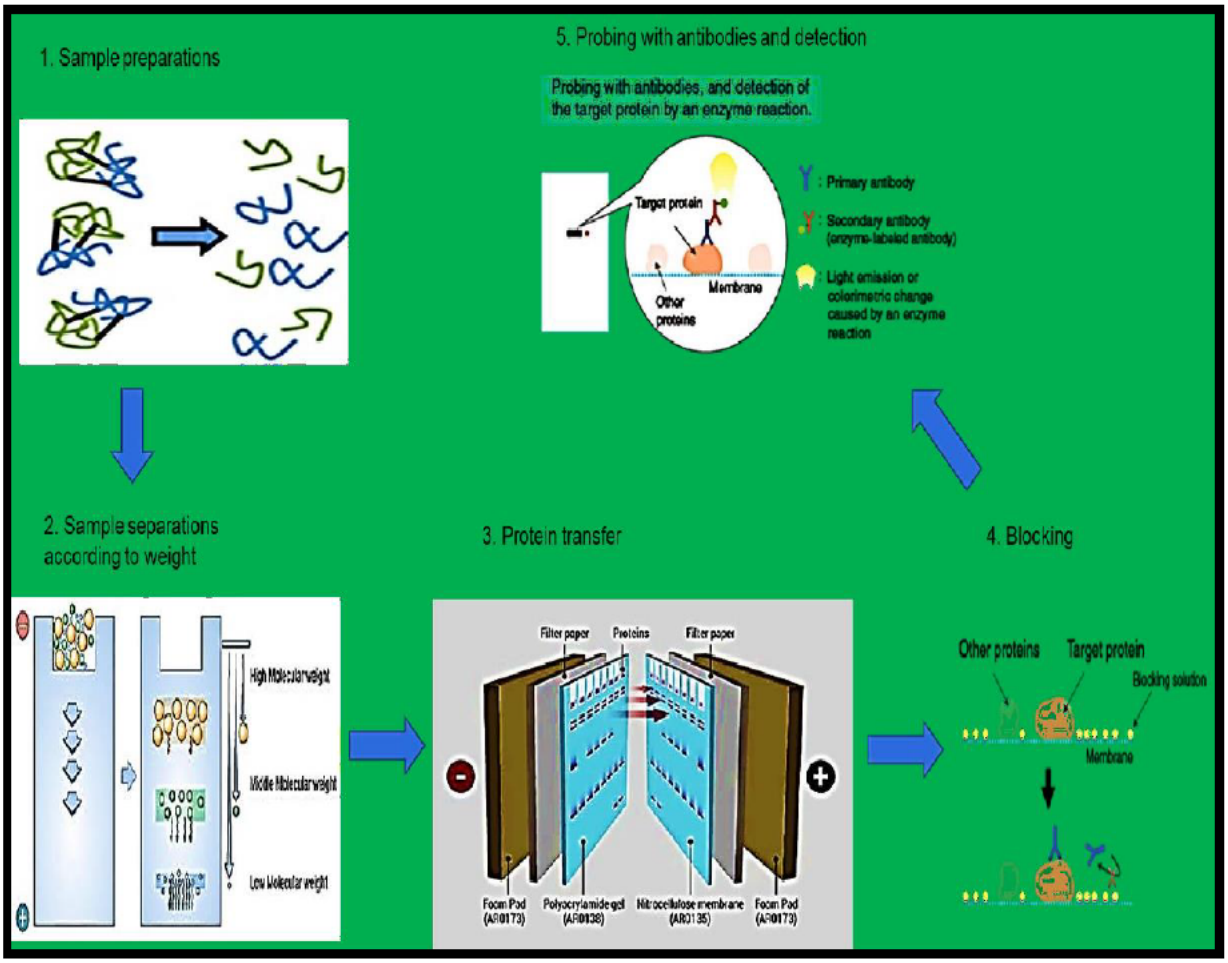

Fig 3.11: Western blot principle (summary). Protein samples separated according to size using SDS-gel are located when the specific antibodies bind and emit detectable light (prepared by the author).

3.12.2. Protocol

Western blot was used to determine protein expression of p53, total and phosphorylated AMPK, whereas, β-actin (Sigma) was used as a housekeeping protein.

3.12.2.1 Sample preparations

Standardised Protein samples were prepared by boiling for 5 minutes in 1x laemmli buffer (distilled water, 0.5M Tris-HCl with a pH of 6.8, 10%SDS, 5% β-mercaptoethanol and 1% bromophenol blue). Following incubation at 100ºC, the samples were allowed to cool at room for temperature and then stored at -20ºC until western blot assay.

3.12.2.2 SDS-PAGE

Gels for SDS-PAGE were prepared using the Mini-PROTEAN Tetra Cell casting frame (Bio-Rad). Thereafter, a 10% resolving gel (distilled water (dH_2O), Tris (1.5M, pH 8.8), 10% SDS, Bis-acrylamide, ammonium persulphate (APS) and Tetramethylenediamine (TEMED)) was prepared and allowed to polymerise for 1 hr. Following polymerisation, a 4% stacking gel (dH_2O, Tris (0.5M, pH 6.8), 4% SDS, Bis-acrylamide, APS and TEMED) was prepared and cast on top of resolving gel. A 1cm plastic comb was placed between the glass plates to allow the formation of wells and the gel was allowed to set for 30-40 min.

Once the stacking gel was set, the gel cassettes were transferred into the electrode assembly and placed in the electrode tank (Mini-PROTEAN Tetra Cell System, Bio-Rad). Running buffer (25mM Tris, 192mM glycine and 0.1% SDS) was poured into the electrode tank. Protein samples (25µl) along with a molecular weight marker (5µl; Precision Plus Protein All Blue Standards, catalogue no. #161-0373, Bio-Rad) was loaded into the wells of the gel, and the samples were electrophoresed at 150V for 1hr using a compact power supply (Bio-Rad).

3.12.2.3 Western blotting

Following electrophoresis, the gels were removed from the glass plates. The fiber pads, nitrocellulose membrane, and gels were equilibrated in transfer buffer (25mM Tris, 191.8mM glycine and 20% methanol) for 10 min. A gel sandwich consisting of a fiber pad, nitrocellulose membrane, gel, and fiber were placed between the electrodes of the transfer apparatus. The separated proteins were electro-transferred onto the nitrocellulose membrane using the Bio-Rad Trans-Blot Turbo Transfer System for 30 min at 20V.

The membranes were blocked after the transfer process in 5ml of blocking solution which consisted of 5% BSA and Tween 20-Tris buffered saline (TTBS: 150mM NaCl, 3mM KCl, 25mM Tris, 0.05% Tween 20, dH_2O, pH 7.5) for 1 hr at room temperature with gentle shaking in order to prevent non-specific binding of primary antibodies. Membranes were then immuno-probed with primary antibodies (1:1000 dilution in 5% BSA) against p53, phosphorylated AMPK and total AMPK. The membranes were then placed on a shaker for 1 hr at room temperature, and this was followed by overnight incubation at 4^oC. After overnight incubation, the membranes were washed 5 times for 10 min with TTBS and then incubated with HRP-conjugated secondary antibody for 1 hr at room temperature. Subsequently, the

secondary antibody was discarded, and membranes were washed (3 times;10 min). Protein bands were visualized using Clarity Western ECL Substrate kit (Bio-Rad). Images were captured using the ChemiDoc™ XRS+ Molecular Imaging System (Bio-Rad).

Membranes were quenched using 5% hydrogen peroxide, incubated in 5% BSA (1hr; room temperature), rinsed 5 times with wash buffer (TTBS) and probed with an HRP-conjugated antibody for the housekeeping protein (β-actin). The Image Lab Software version 5.1 (Bio-Rad) was used to analyse protein expression. Protein expression was normalised by dividing the RBD of the protein of interest by the RBD of β-actin. The results were expressed as relative band density compared to the control.

3.13 Lactate Dehydrogenase (LDH) Assay

3.13.1 Principle

Lactate dehydrogenase (LDH) is an oxidoreductase enzyme that catalyses the interconversion of lactate and pyruvate. It is found in the cytoplasm of all cells and is rapidly released into the cell culture medium during plasma membrane damage/injury. Thus, its release is considered an early biomarker for determining membrane integrity. The release of LDH is also considered an early stage of necrosis but a late event of apoptosis (Parhamifar, et al., 2013). The LDH assay is a non-radioactive colourimetry test used to access cell membrane integrity/damage. This assay is based on measuring LDH released by damaged cells. LDH activity is easily quantified using NADH. The NADH production is catalysed by LDH through the reduction of NAD+ to NADH in the presence of L-lactase during the conversion of lactase to pyruvate. The production of NADH is measured in a coupled reaction in which a yellow tetrazolium salt INT is reduced into a red coloured-formazan that is easily quantified. A spectrophotometer can then be used to measure the absorbance of formazan at 492nm-500nm. The intensity of the formazan produced is directly proportional to the LDH enzyme activity, which is directly proportional to the number of damaged cells (Kumar, et al., 2018).

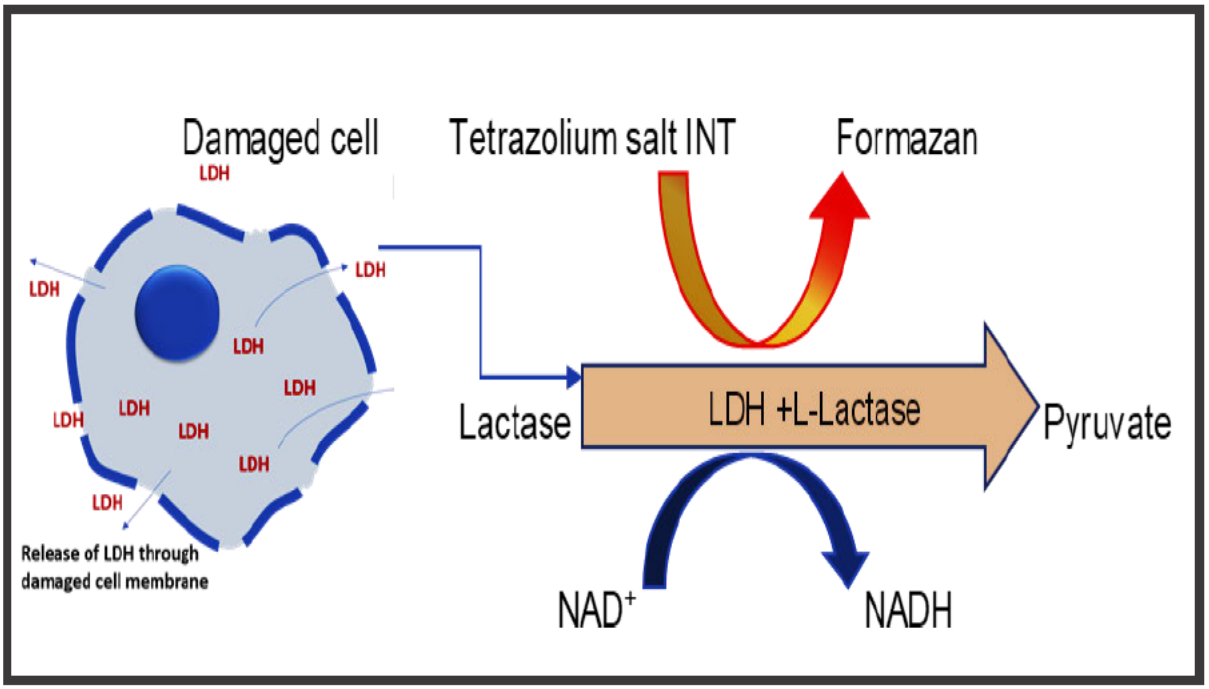

Fig 3.12: Principle of the LDH assay. A yellow tetrazolium INT is reduced into a red formazan in a coupled reaction when LDH catalyses the production of NADH in the presence of L-Lactase during the process of interconversion of lactase into pyruvate (Prepared by the author).

3.13.2 Protocol

Following treatment of HepG2 cells for 24 hrs, the supernatants were removed and used to determine LDH activity. Briefly, 100µl supernatant and 100µl LDH reagent (Roche, Mannheim, Germany) which comprises of catalyst (diaphorase/NAD+) and dye solution (INT/sodium lactate) was added in triplicate in a 96-well microtiter plate. The plate was then incubated at room temperature in the dark for 30 min. The optical density was measured using a spectrophotometer at 500nm.

3.14 Statistical analysis

Microsoft Excel 2016 and GraphPad Prism version 5.0 (GraphPad Software Inc., California) was used to perform all statistical analyses. The one-way analysis of variance (ANOVA) with the Bonferroni multiple comparisons test was used to analyse all data. Results were represented as the mean ± standard deviation, unless otherwise stated. A value of $p<0.05$ was considered statistically significant.

CHAPTER 4: RESULTS

4.1 FA and FB_1 decreased HepG2 cell viability

The MTT assay was used to determine cell viability in HepG2 cells following co-treatment with various concentrations (0.25-50μM) of FA and FB_1 for 24 hrs that resulted in a dose-response curve. An IC_{50} of 27μM was obtained using a graph pad (Fig 4.1).

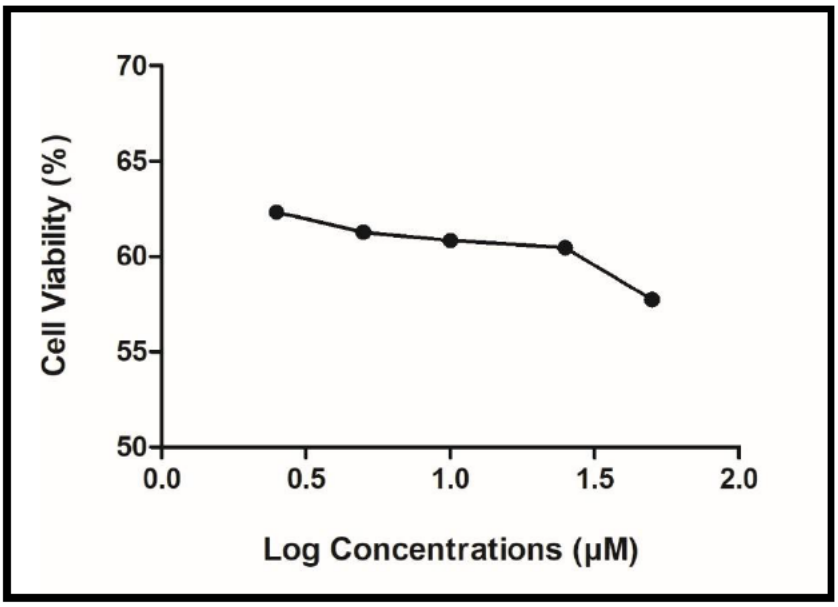

Fig 4.1: A dose-dependent decrease in HepG2 cell viability after co-treatment with different concentrations (0.25, 5, 10, 25 and 50μM) of FA and FB_1 for 24hrs.

4.2 FA and FB_1 altered ATP levels in HepG2 cells

The ATP concentrations were determined in FA and FB_1 co-treated cells in relation to the untreated control. FA and FB_1 co-treatment significantly increased ATP levels at 5μM and 27μM; however, at 100μM and combined IC_{50}s the levels of ATP were significantly decreased (***p<0.0001), (Fig 4.2).

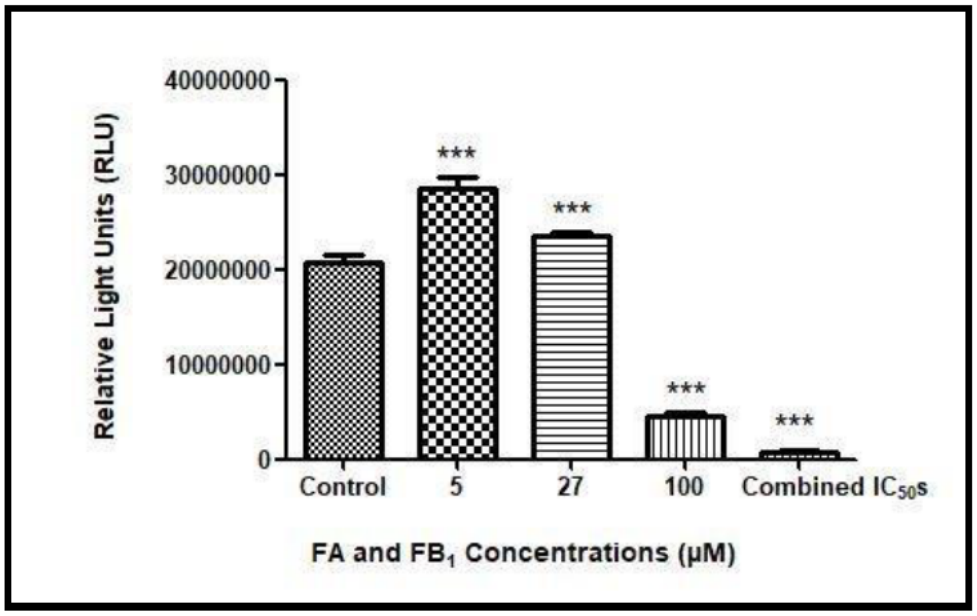

Fig 4.2: ATP levels in FA and FB_1 co-treated HepG2 cells. Data denotes mean and +/- standard deviation. Number of replicates (n)=3.

4.3 FA and FB_1 Damaged HepG2 Cell Membranes

Due to the alteration in ATP levels in the FA and FB_1 treated cells, the LDH assay was performed to determine the effect of FA and FB_1 on cell membrane integrity. In addition, elevated levels of LDH are an indication of cytotoxicity, damaged cell membrane, late apoptosis, and early necrosis. The co-treatment indicated a significant increase in LDH levels at high concentrations and a decrease in LDH levels at the lower concentrations compared to the control. Results are represented in the Fig 4.3 (**$p<0.005$ and ***$p<0.0001$).

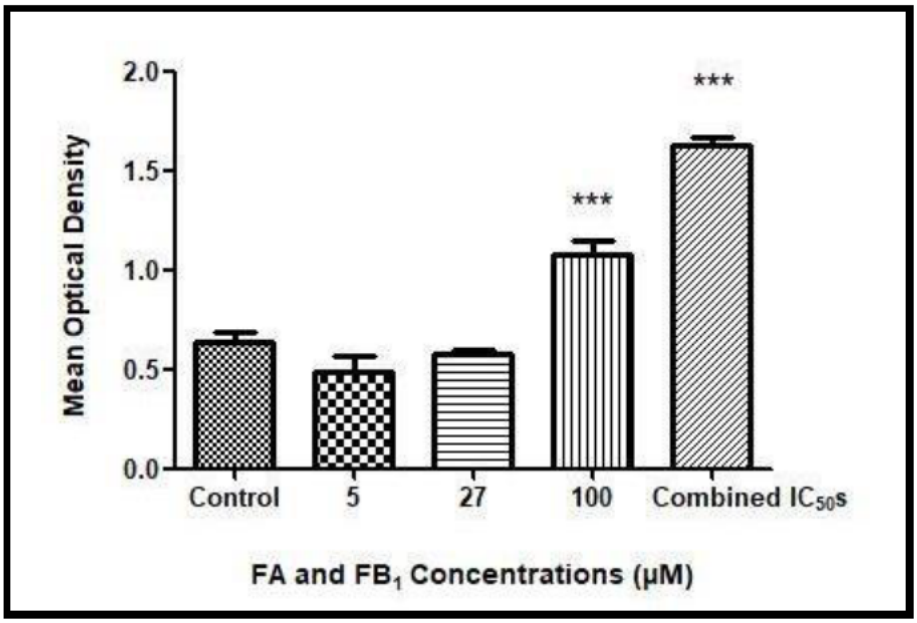

Fig 4.3: The effect of FA and FB_1 co-treatment on LDH leakage in HepG2 cells. Data represent mean and +/- standard deviation (n=3).

4.4 FA and FB_1 Induced Oxidative Stress in HepG2 Cells

The TBARS assay is used to quantify MDA, a by-product of lipid peroxidation and a molecular indicator of oxidative stress. FA and FB_1 co-treatments dose-dependently increased the concentration of MDA and hence oxidative stress in HepG2 cells compared to the control (**p<0.005 and ***p<0.0001), (Fig 4.4).

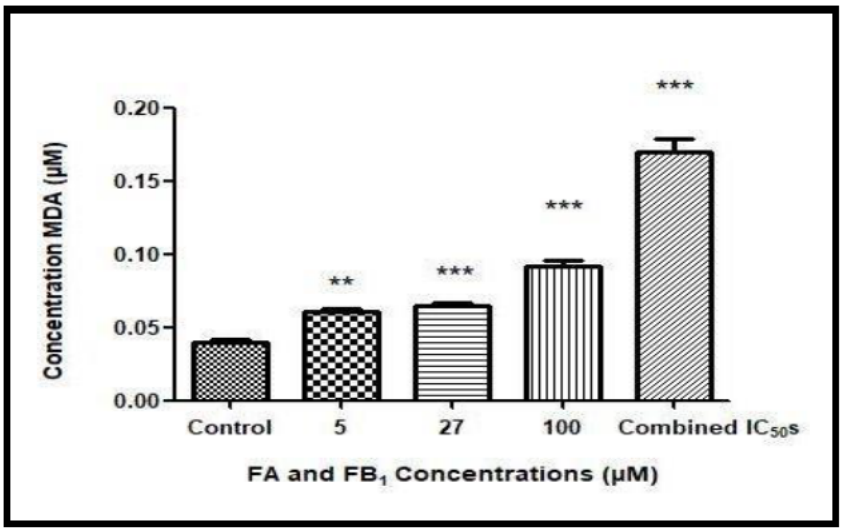

Fig 4.4: The effect of FA and FB_1 co-treatment on oxidative stress in HepG2 cells. Data signifies mean and +/- standard deviation (n=3).

4.5 FA and FB_1 Altered the Protein Expression of p-AMPK and total AMPK in HepG2 Cells

AMPK has anti-proliferative functions and it is usually activated in cells experiencing oxidative stress. AMPK protein expressions were determined by western blot in control and co-treated HepG2 cells. FA and FB_1 significantly decreased p-AMPK (B) in relation to control, and total-AMPK. Protein expressions of total AMPK (C) at 5µM was decreased, however, at 27µM, 100µM and combined IC50s the expressions were significantly increased in relation to the control (*p<0.05, **p<0.005 and ***p<0.0001). A represents p-AMPK, total AMPK and β-actin bands.

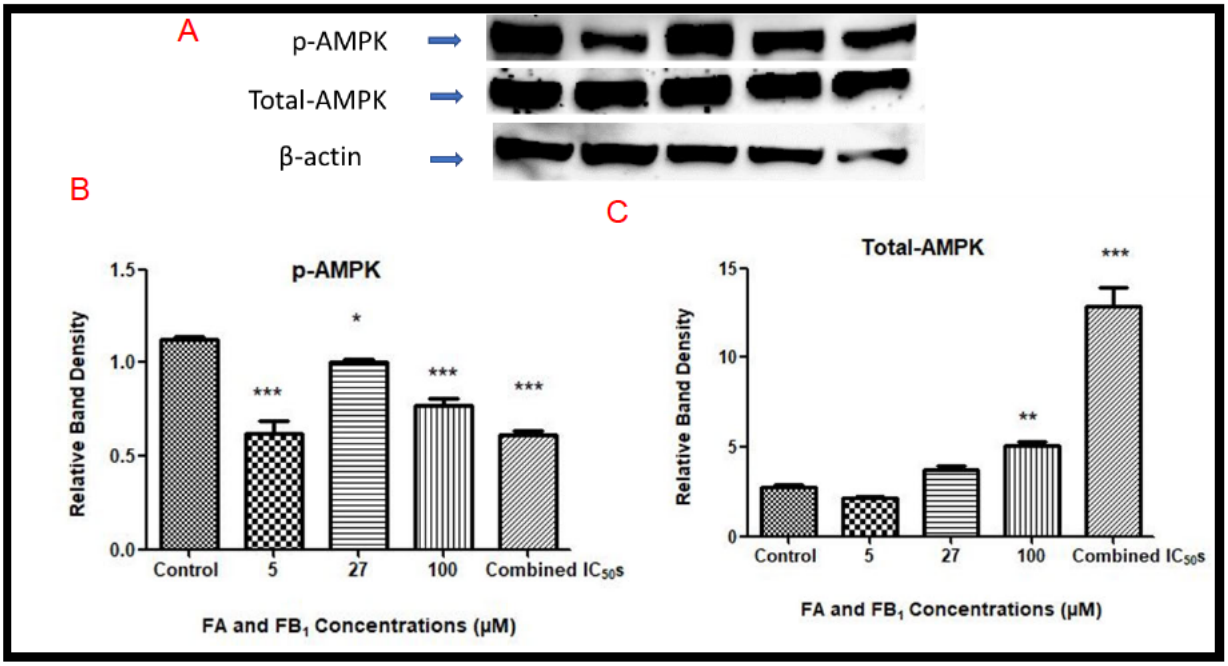

Fig 4.5: The effect of FA and FB_1 co-treatment on the protein expression of AMPK and p-AMPK in HepG2 cells. **A)** p-AMPK, total AMPK and β-actin bands. **B)** graph of FA and FB_1 concentrations vs relative band density. **C)** graph of FA and FB_1 vs relative band density.

4.6 FA and FB_1 Decreased the Protein Expression of p53 In HepG2 Cells

p53 is a tumour suppressor protein that is activated in response to oxidative stress and DNA damage. Western blot was used to determine the protein expression of p53 in HepG2 cells. FA and FB_1 co-treated cells showed a decrease in p53 expression compared to the control, however, the decrease was significant at 5µ,100µ and combined IC_{50}s (*p<0.05, **p<0.005 and ***p<0.0001), (Fig 4.6).

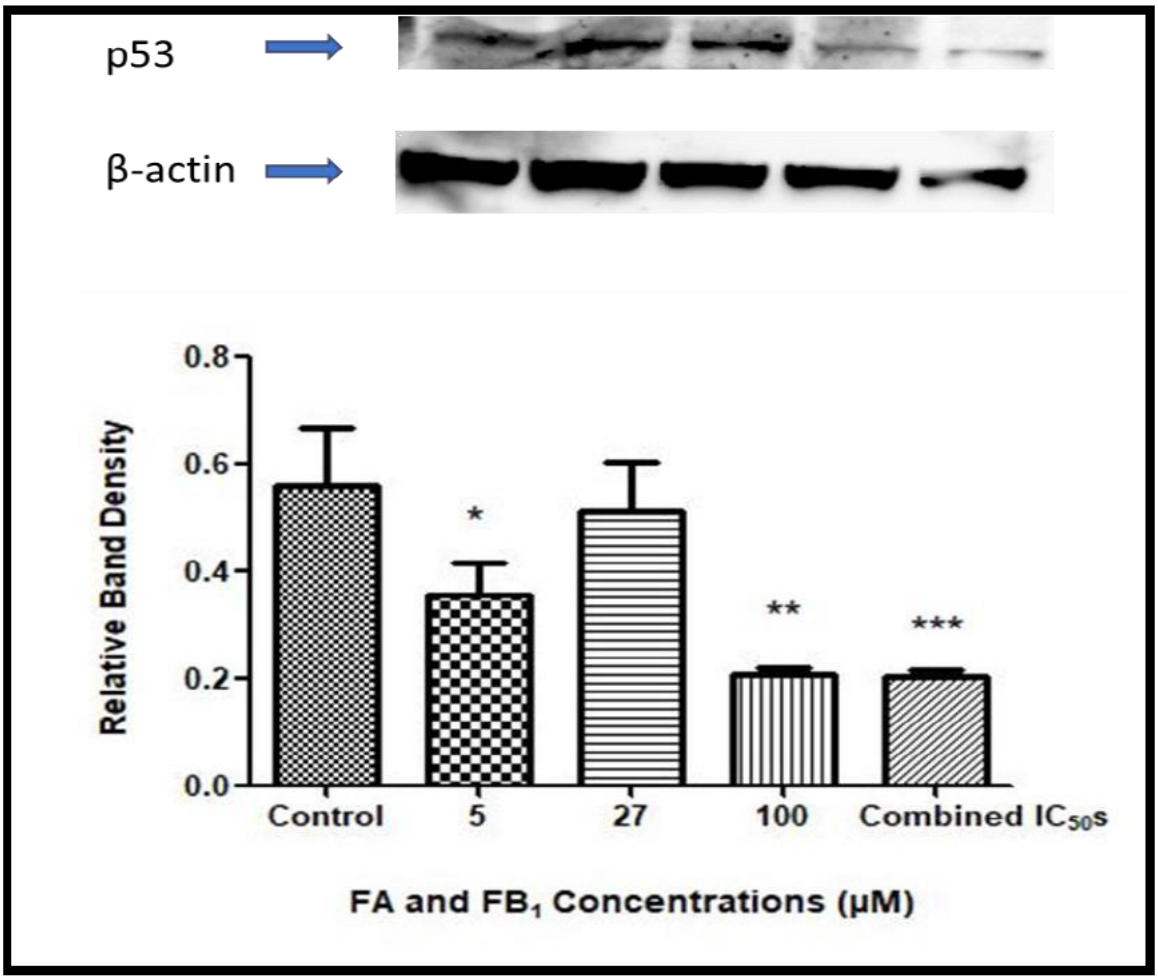

Fig 4.6: The effect of FA and FB_1 co-treatment on p53 protein expression in HepG2 cells.

4.7 FA and FB_1 Increased the mRNA Expression of *FOXO3a* in HepG2 Cells

FOXO3a is involved in the initiation of apoptosis by activating crucial pro-apoptotic molecules that in turn activate and promote the autocleavage of pro-caspases. *FOXO3a* is directly phosphorylated by AMPK during oxidative stress and hence the increase in oxidative stress induced in HepG2 cells when exposed to a combination of FA and FB_1 may affect *FOXO3a* expression. *FOXO3a* mRNA expression was measured using qPCR. HepG2 cells co-treated with FA and FB_1 showed a decreased expression of FOXO3a at 5μM and at combined IC50s, with the decrease being significant at 5μM. FOXO3a mRNA expressions were increased at 27μM and 100μM compared to the control (***$p<0.0001$), (Fig 4.7).

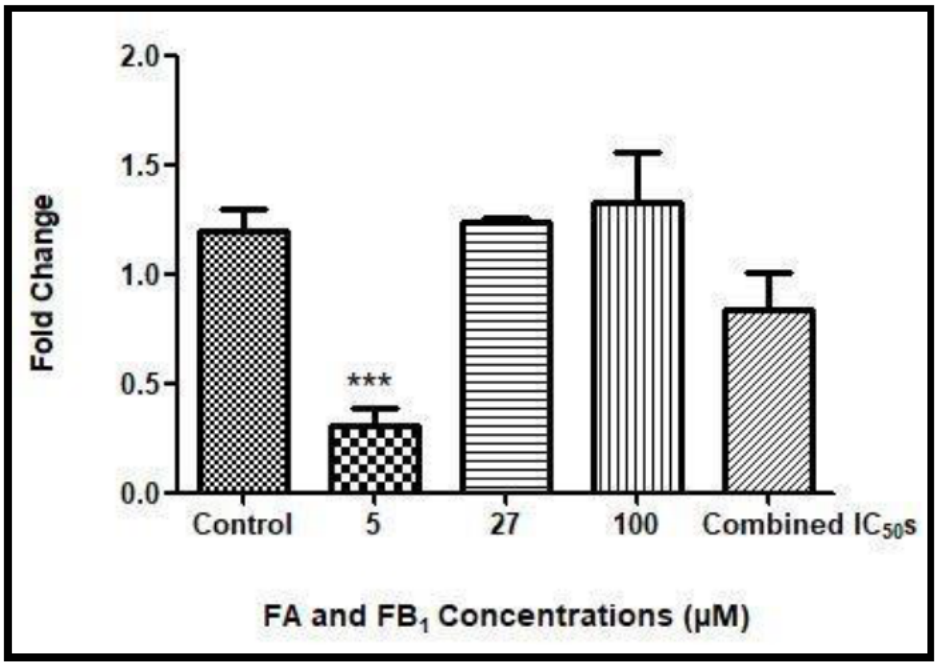

Fig 4.7: The effect of FA and FB_1 co-treatment on *FOXO3a* expression in HepG2 cells.

4.8 FA and FB_1 Regulated apoptosis in HepG2 cells

Following co-treatment of HepG2 cells with FA and FB_1 for 24hrs, the caspase-Glo luminometry assays were used to determine caspase activities. Caspases are important initiators and executioners of apoptosis. Activities of the initiator caspases -8 and -9 as well as the executioner caspase -3/7 were measured.

Figure 4.8 a and b shows that a combination of both FA and FB_1 increased the activities of caspases -8 and -9 at 5-100μM FA and FB_1 treated cells in relation to the control. Cells treated with the combined IC_{50}s indicated a significant decrease in caspase 8 and 9 activities. FA and FB_1 increased activities of caspase-3/7 (c) at 5-100μM in a dose-dependent manner. At combined IC_{50}s, caspase -3/7 is significantly decreased (***$p<0.0001$).

a. Caspase 8 activity

b. Caspase 9 activity

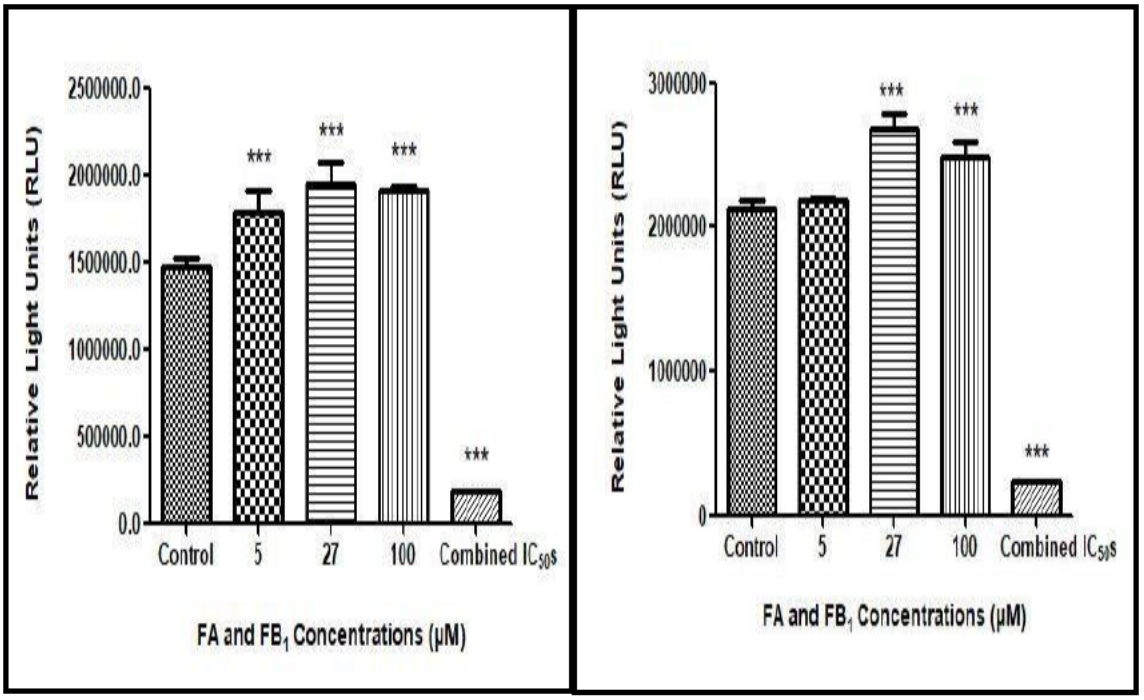

c. Caspase 3/7 activity

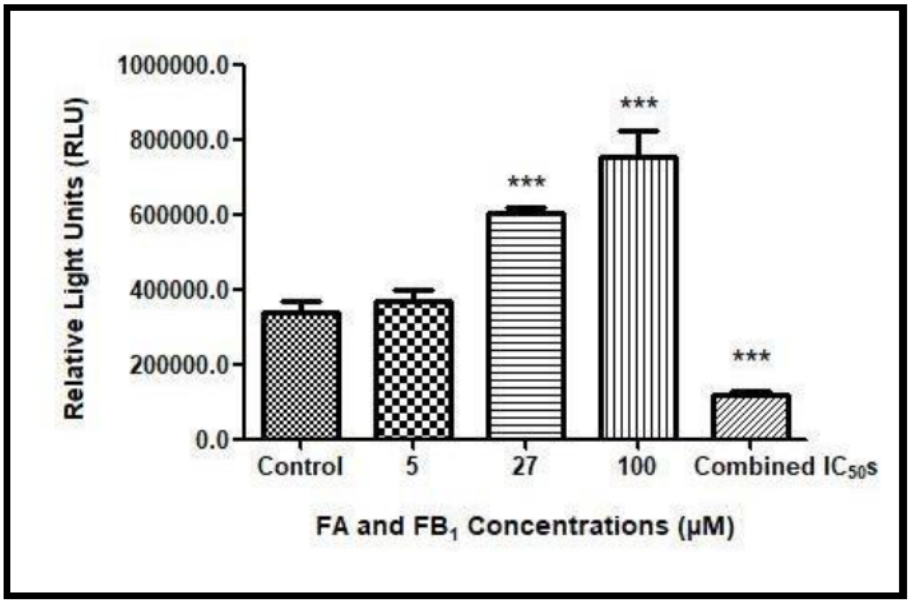

Fig 4.8: The effect of FA and FB_1 co-treatment on caspase activity in HepG2 cells. **A)** graph of FA and FB_1 vs relative light units (caspase 8 activity). **B)** graph of FA and FB_1 concentrations vs relative light units (caspase 9 activity). **C)** FA and FB_1 concentrations vs relative light units (caspase 3/7 activity).

CHAPTER 5: DISCUSSION

Mycotoxins are secondary metabolites produced by *Fusarium* species and found on plants, and at times in co-existence. FA and FB_1 are co-produced by the *Fusarium* species and contaminate foods and animal feeds worldwide. They are frequently found on maize and maize-based foods and feeds. Individually, these mycotoxins have been shown to induce toxicity in humans and animals; however, studies evaluating their possible synergistic interactions are limited. In this study, we aimed to evaluate possible synergistic effects of FA and FB_1 on human liver (HepG2) cells following a 24hr exposure. This was conducted by investigating the effects of a combination of FA and FB_1 on apoptosis following the AMPK signalling pathway in HepG2 cells.

It is essential to determine the synergistic interaction between FA and FB_1 in humans and animals as these mycotoxins are often co-produced on maize and other agricultural foods and are most likely to be ingested together.

The liver, due to its close relationship with the gastrointestinal tract, is the major site of biotransformation and detoxification of drugs and chemical substances including mycotoxins. Combination of mycotoxins can have synergistic, antagonistic, or additive effects depending on the dose and/or length of exposure of the mycotoxin, therefore implying the need to study a combination of mycotoxins especially those found on world staple foods such as maize (Li, et al., 2014). FA decreased HepG2 cell viability in a dose-dependent with a reported IC_{50} value of 104µg/ml (Abdul, et al., 2016; Ghazi, et al., 2017). Additional studies focusing on FB_1 toxicity in the HepG2 cells, indicated that FB_1 also reduced cell viability in a dose-dependent manner with an IC_{50} of 200µM (Chuturgoon, 2014). The present study provides data on the combined effects of FA and FB_1 on HepG2 cell viability and apoptosis via the AMPK signalling pathway. The results showed that a combination of FA and FB_1 decreased HepG2 cell viability in a dose-dependent manner with an IC_{50} of 27µM (Fig 4.1). This IC_{50} is much lower than that of the individual treatments and therefore, by implication that FA and FB_1 may have synergistic interactions in the liver HepG2 cells. Further, co-treatment of HepG2 cells with FA and FB_1 is more toxic than that of the individual treatments.

An increase in cellular ROS both by FA and FB_1 was shown to induce cytotoxicity. The high reactivity of ROS is the result of an unpaired electron and are usually formed in the mitochondria as a natural by-product of normal metabolism. ROS is important for normal biological functions such as cell signalling and homeostasis; however, excess ROS is detrimental to the cell. Mycotoxins increase ROS levels drastically leading to oxidative stress (Silva, et al., 2018); in this study, ROS levels increased in a dose dependent manner (Fig

4.4). Studies have shown that FA toxicity is due to its ability to chelate metal cations (Bacon, et al., 1995). The toxicity of FA in cells induces the synthesis of ROS (Singh et al., 2014). A study conducted by Blacutt, et al., (2017) also demonstrated that FB_1 caused cytotoxicity by inhibiting the production of ceramide. The overproduction of ROS results in oxidative damage (Yuan et al., 2019). The excessive ROS due to exposure of cells to mycotoxins (FA or FB_1) reacts with unsaturated lipids and results in lipid peroxidation. The lipid peroxide is then metabolised into a toxic MDA. FA and FB_1 co-treatment showed a significant increase in MDA in a dose-dependent manner (Fig 4.4).

Previously, both FA and FB_1 were shown to independently increase oxidative stress that led to cell death (Singh, et al., 2014; Blacutt et al., 2017). Apoptosis is a physiological process triggered by extrinsic or intrinsic cell death signals. It has a role in maintaining homeostasis and eliminates damaged and dysfunctional cells. Apoptosis is an ATP-dependent process that involves caspase activation. Therefore, to determine whether apoptosis occurred due to FA and B1 exposure, caspase activities were measured. It was reported that FA induced apoptosis in SNO oesophageal cancer cells by increasing the activity of caspase -9, -8 and -3/7, and BAX expression whilst ATP levels and BCL-2 expressions were decreased (Devnarain, et al., 2017).

FA and FB_1 co-treatments demonstrated an increase in caspase -8 and -9 activities at 5-100µM concentrations in relation to the control (Figs. 4.8 a and b). However, at combined IC_{50}s, the activities of both caspases -8 and -9 were significantly decreased. Additionally, the activity of caspase-3/7 was significantly increased at 5-100µM (Fig 4.8c). However, at the combined IC_{50}s the activity of caspase-3/7 was decreased compared to the control. This study further assessed the concentration of ATP; ATP was significantly increased at 5 µM and 27µM (FA and FB_1 co-treatment) but decreased at 100µM and the combined IC_{50}s (fig4.2). A decrease in ATP and caspase activity is usually demonstrated in cells switching from one type of cell death (apoptosis) to another (e.g. necrosis). Necrosis depletes ATP and can occur with limited caspase involvement or its absence thereof (Elmore, 2005; Zamaraeva, et al., 2005).

Lactate dehydrogenase (LDH) assay was conducted to determine LDH leakage. LDH is released from the cell through a damaged cell membrane. LDH release is an indicator of late apoptosis or early necrosis (Parhamifar, et al., 2013). The LDH results indicated a significant reduction in LDH levels at 5µM and 27µM FA and FB_1, and a significant increase at 100µM and combined IC_{50}s (fig4.3). Overall, the results (caspases -8, -9, -3/7, ATP and LDH) from the combination of FA and FB_1 co-treatments at lower concentrations (5µM and 27µM), suggests that the cells may be at an early stage of apoptosis, however, at 100uM there

might be a late stage of apoptosis and at combined IC_{50}s, FA and FB_1 may have induced early stage of necrosis. The intrinsic pathway and extrinsic pathway are linked and the molecules from one pathway can influence the other (Elmore, et al., 2005). The results showed that both the extrinsic and intrinsic apoptotic pathways were initiated (Figs 4.8a and 4.8b).

AMP-activated protein kinase is known as a master regulator of energy status due to its ability to sense and control the cellular energy status. Its activation by AMP and ADP dependent pathway involve a conformational change within its heterotrimeric complex (Pellose, et al., 2019). However, studies have shown that AMPK can be activated by increased cellular ROS independent of intracellular ATP levels (Jeon, 2016). Oxidative stress activates AMPK by directly inducing oxidation of AMPK cysteine residues (Auciello, et al., 2014; Jeon 2016). AMPK was previously shown to have anti-proliferative functions; however, this depends on the type of cell. It directly inhibits oncogene phosphorylation and promotes the phosphorylation of tumour suppressor genes (e.g. p53) and *FOXO3a* (El-Masry, et al., 2015). *FOXO3a* and p53 play a role in activating pro-apoptotic molecules and inhibiting anti-apoptotic molecules. *FOXO3a* activates and induces the expression of BIM and stimulates the expression of death receptor ligands whereas p53 activates BID and BAX (Frank, et al., 2015; Su, et al., 2015). Therefore, in this study, the role of AMPK-*FOXO3a* and AMPK-p53 in apoptosis were investigated. The protein expression of total AMPK at 5µM was decreased whereas at 27µM, 100µM and at combined IC_{50}s it was significantly increased compared to control. Despite an increase in total AMPK protein expressions, the expression of phosphorylated AMPK was decreased (fig4.5). The p53 protein expression was significantly decreased in all co-treated samples compared to the control (fig4.6). The *FOXO3a* mRNA expression was decreased at 5µM and combined IC_{50}s and increased at 27µM and 100µM when compared to the control (fig4.7). An inverse relationship exists between total AMPK and ATP. The total AMPK expressions were increased when ATP levels were decreased and vice versa.

p53 is activated in response to DNA damage and oxidative stress, therefore, leading to cell cycle arrest and apoptosis (Su, et al., 2015). It is a zinc-dependent metalloprotein. The zinc ion is important in the maintenance of p53 wild type structural stability. The zinc ion is coordinated by a histidine (His179) and three cysteine side chains (Cys176, Cys238, and Cys242), (Joerger and Fersht, 2007). Our results showed that FA and FB_1 co-treated cells had decreased p53 protein expression when compared to the untreated control (fig4.9) and this may occur due to the chelating ability of FA. Similar results were observed by Ghazi, et al., (2017) in which FA (580.32uM) decreased the protein expression of p53 in HepG2 cells in relation to the control. The removal of the zinc ion by a metal chelating agent such as FA

results in destabilised p53 protein, therefore, causing structural perturbations and loss of sequence-specific DNA binding sites (Joerger and Fersht 2007). The decrease in p53 protein indicates a direct relationship with p-AMPK. This decrease might be because p-AMPK couldn't activate p53 as it was also suppressed. Another study reported that a decrease in p53 protein expression is due to its constitutive degradation (Antunes, et al., 2015). The degradation is due to the impairment of the AKT pathway which normally signals for p53 to stabilise in response to DNA damage. A recent study reported that the p53 protein expression was significantly increased, however the samples were treated with FB_1 for 2, 3 and 4 days. The samples treated for 24 hrs with FB_1 indicated no significant increase in mice colon tissue (Kim, et al., 2018).

5.1 Limitations and future work

This *in vitro* experimental study on HepG2 cells was used to investigate oxidative stress and cell death after co-exposure to FA and FB_1 for 24 hrs. *In vitro* models enable cells to be isolated from any other type of influence, thereby, determining the potential effect of mycotoxins on the cells without any external confounding factors; however, the lack of complexity, multicellularity, and an organ system are major disadvantages. *In vivo* animal models, due to their complexity, multicellularity, and presence of functional organ systems, are more reliable models for toxicity testing as they mimic that of the human system. Hence, future work would involve testing the effect of FA and FB_1 co-exposure in an *in vivo* mice model. In addition, the maximum time period used in this study was 24 hrs. Many proteins and stress pathways respond differently to toxins under acute, sub-chronic, and chronic conditions, therefore in the future, the effects of FA and FB_1 co-treatment will be investigated at 6, 48 and 72 hrs.

The effects of FA and FB_1 co-treatment were only assessed on tumour suppressor, p53 and transcription factor FOXO3a. The effects on oncogenes such as AKT which regulate the expressions of p53 will be included in the future work. Epigenetic modifications such as DNA methylation, histone methylation and microRNAs also play a major role in toxicology and adverse cellular outcomes; hence the effect of FA and FB_1 co-treatment on epigenetic modifications will be determined.

CHAPTER 6: CONCLUSION

The mycotoxins, FA and FB_1 frequently contaminate agricultural foods posing a serious health hazard to humans and animals. To date several studies have evaluated the individual toxic effects of these mycotoxins; however, their combined effects are unclear. In this study, FA and FB_1 co-treatment downregulated AMPK signalling and induced apoptosis in HepG2 cells. The data further suggests that the combination of these mycotoxins inhibits the phosphorylation of AMPK at the activation loop of threonine 172 (THR-172) of the α-subunit in spite of an increase in the total AMPK protein expression. p-AMPK suppressions may explain a decrease in p53 protein expression.

In addition, the dose-dependent increase in oxidative stress caused cell membrane damage as shown by the significant increase in LDH leakage and indicated that FA and FB_1 co-treatment induced cell death via necrosis, however, at low concentrations, the cells undergo apoptosis, as evidenced by the increase in caspase (-8, -9, and -3/7) activities as well as ATP and LDH levels. These findings are important as they provide information on the toxic synergistic interaction between FA and FB_1 in human cells.

REFERENCE

Abdul, N.S., Nagiah, S. and Chuturgoon, A.A., (2016). Fusaric acid induces mitochondrial stress in human hepatocellular carcinoma (HepG2) cells. *Toxicon*, *119*: 336-344.

Ali, N., Sardjono, Yamashita, A. and Yoshizawa, T., (1998). Natural co-occurrence of aflatoxins and Fusavium mycotoxins (fumonisins, deoxynivalenol, nivalenol and zearalenone) in corn from Indonesia. *Food Additives & Contaminants*, *15*(4): 377-384.

Alto mare, D.A. and Testa, J.R., (2005). Perturbations of the AKT signaling pathway in human cancer. *Oncogene*, *24*(50): 7455.

Antunes, A.T., Goos, Y.J., Pereboom, T.C., Hermkens, D., Wlodarski, M.W., Da Costa, L. and MacInnes, A.W., (2015). Ribosomal protein mutations result in constitutive p53 protein degradation through impairment of the AKT pathway. *PLoS genetics*, *11*(7): 1005326.

Aslantürk, Ö.S., 2018. *In Vitro Cytotoxicity and Cell Viability Assays: Principles, Advantages, and Disadvantages* (Vol. 2, p. 64). InTech.

Auciello, F.R., Ross, F.A., Ikematsu, N. and Hardie, D.G., (2014). Oxidative stress activates AMPK in cultured cells primarily by increasing cellular AMP and/or ADP. *FEBS letters*, *588*(18): 3361-3366.

Bacon, C.W., Porter, J.K. and Norred, W.P., (1995). Toxic interaction of fumonisin B 1 and fusaric acid measured by injection into fertile chicken egg. *Mycopathologia*, *129*(1): 29-35.

Belyi, V.A., Ak, P., Markert, E., Wang, H., Hu, W., Puzio-Kuter, A. and Levine, A.J., (2010). The origins and evolution of the p53 family of genes. *Cold Spring Harbor perspectives in biology*, *2*(6): 001198.

Blacutt, A.A., Gold, S.E., Voss, K.A., Gao, M. and Glenn, A.E., (2018). Fusarium verticillioides: Advancements in understanding the toxicity, virulence, and niche adaptations of a model mycotoxigenic pathogen of maize. *Phytopathology*, *108*(3): 312-326.

Bochner, B.R., Huang, H.C., Schieven, G.L. and Ames, B.N., (1980). Positive selection for loss of tetracycline resistance. *Journal of bacteriology*, *143*(2): 926-933.

Bouizgarne, B., El-Maarouf-Bouteau, H., Frankart, C., Reboutier, D., Madiona, K., Pennarun, A.M., Monestiez, M., Trouverie, J., Amiar, Z., Briand, J. and Brault, M., (2006). Early physiological responses of Arabidopsis thaliana cells to fusaric acid: toxic and signalling effects. *New Phytologist*, *169*(1): 209-218.

Brady, C.A. and Attardi, L.D., (2010). p53 at a glance. *J Cell Sci*, *123*(15): 2527-2532.

Brown, D.W., Butchko, R.A., Busman, M. and Proctor, R.H., (2012). Identification of gene clusters associated with fusaric acid, fusarin, and perithecial pigment production in Fusarium verticillioides. *Fungal Genetics and Biology*, *49*(7): 521-532.

Bryden, W.L., (2012). Mycotoxin contamination of the feed supply chain: Implications for animal productivity and feed security. *Animal Feed Science and Technology*, *173*(1-2): 134-158.

Cardaci, S., Filomeni, G. and Ciriolo, M.R., (2012). Redox implications of AMPK-mediated signal transduction beyond energetic clues. *J Cell Sci*, *125*(9): 2115-2125.

Carter, M. and Shieh, J.C., (2015). *Guide to research techniques in neuroscience*. Academic Press.

Chang, D.W., Xing, Z., Capacio, V.L., Peter, M.E. and Yang, X., (2003). Interdimer processing mechanism of procaspase-8 activation. *The EMBO journal*, *22*(16): 4132-4142.

Chuturgoon, A.A., Phulukdaree, A. and Moodley, D., (2014). Fumonisin B1 modulates expression of human cytochrome P450 1b1 in human hepatoma (Hepg2) cells by repressing Mir-27b. *Toxicology letters*, *227*(1): 50-55.

Chuturgoon, A., Phulukdaree, A. and Moodley, D., (2014). Fumonisin B1 induces global DNA hypomethylation in HepG2 cells–An alternative mechanism of action. *Toxicology*, *315*: 65-69.

Courageot, M.P., Catteau, A. and Despres, P., (2003). Mechanisms of dengue virus-induced cell death. *Adv Virus Res*, *60*: 157-186.

Crutcher, F.K., Liu, J., Puckhaber, L.S., Stipanovic, R.D., Duke, S.E., Bell, A.A., Williams, H.J. and Nichols, R.L., (2014). Conversion of fusaric acid to fusarinol by Aspergillus tubingensis: a detoxification reaction. *Journal of chemical ecology*, *40*(1): 84-89.

Crutcher, F.K., Puckhaber, L.S., Bell, A.A., Liu, J., Duke, S.E., Stipanovic, R.D. and Nichols, R.L., (2017). Detoxification of fusaric acid by the soil microbe Mucor rouxii. Journal of agricultural and food chemistry, 65(24): 4989-4992.

Da Silva, E.O., Bracarense, A.P.F.L. and Oswald, I.P., (2018). Mycotoxins and oxidative stress: where are we?. *World Mycotoxin Journal*, *11*(1): 113-134.

Das, T.P., Suman, S., Alatassi, H., Ankem, M.K. and Damodaran, C., (2016). Inhibition of AKT promotes FOXO3a-dependent apoptosis in prostate cancer. *Cell death & disease*, *7*(2): 2111.

Devnarain, N., Tiloke, C., Nagiah, S. and Chuturgoon, A.A., (2017). Fusaric acid induces oxidative stress and apoptosis in human cancerous oesophageal SNO cells. *Toxicon*, *126*: 4-11.

Dhani, S., Nagiah, S., Naidoo, D.B. and Chuturgoon, A.A., (2017). Fusaric Acid immunotoxicity and MAPK activation in normal peripheral blood mononuclear cells and Thp-1 cells. *Scientific reports*, *7*(1): 3051.

Donato, M.T., Tolosa, L. and Gómez-Lechón, M.J., (2015). Culture and functional characterization of human hepatoma HepG2 cells. In *Protocols in In Vitro Hepatocyte Research*. Humana Press, New York, NY: pp. 77-93

Driehuis, F., (2011). Occurrence of mycotoxins in silage. In *Proceedings of the II International Symposium*.

El-Masry, O.S., Al-Sakkaf, K., Brown, B.L. and Dobson, P.R., (2015). Differential crosstalk between the AMPK and PI3K/Akt pathways in breast cancer cells of differing genotypes: leptin inhibits the effectiveness of AMPK activation. *Oncology reports*, *34*(4): 1675-1680.

Elmore, S., (2007). Apoptosis: a review of programmed cell death. *Toxicologic pathology*, *35*(4): 495-516.

Fandohan, P., Hell, K., Marasas, W.F.O. and Wingfield, M.J., (2003). Infection of maize by Fusarium species and contamination with fumonisin in Africa. *African Journal of Biotechnology*, *2*(12): 570-579.

Fernandez-Pol, J.A., Fernandez-Pol and Jose Alberto, (1998). *Antiviral agent*. U.S. Patent 5,767,135.

Ferrari, D., Stepczynska, A., Los, M., Wesselborg, S. and Schulze-Osthoff, K., (1998). Differential regulation and ATP requirement for caspase-8 and caspase-3 activation during CD95-and anticancer drug–induced apoptosis. *Journal of Experimental Medicine*, *188*(5): 979-984.

Frank, D.O., Dengjel, J., Wilfling, F., Kozjak-Pavlovic, V., Häcker, G. and Weber, A., (2015). The pro-apoptotic BH3-only protein Bim interacts with components of the translocase of the outer mitochondrial membrane (TOM). *PLoS One*, *10*(4): 0123341.

Fridman, J.S. and Lowe, S.W., (2003). Control of apoptosis by p53. *Oncogene*, *22*(56): 9030.

Furukawa-Hibi, Y., Kobayashi, Y., Chen, C. and Motoyama, N., (2005). FOXO transcription factors in cell-cycle regulation and the response to oxidative stress. *Antioxidants & redox signaling*, *7*(5-6): 752-760.

Gafni, J., Cong, X., Chen, S.F., Gibson, B.W. and Ellerby, L.M., (2009). Calpain-1 cleaves and activates caspase-7. *Journal of Biological Chemistry*, *284*(37): 25441-25449.

Gao, B., Jeong, W.I. and Tian, Z., (2008). Liver: an organ with predominant innate immunity. *Hepatology*, *47*(2): 729-736.

Gaumann, E., (1958). The mechanisms of fusaric acid injury. *Phytopathology*, *48*(12): 670-686.

Ghazi, T., Nagiah, S., Tiloke, C., Sheik Abdul, N. and Chuturgoon, A.A., (2017). Fusaric acid induces DNA damage and post-translational modifications of p53 in human hepatocellular carcinoma (HepG2) cells. *Journal of cellular biochemistry*, *118*(11): 3866-3874.

Ghazi, T., Nagiah, S., Naidoo, P. and Chuturgoon, A.A., (2019). Fusaric acid-induced promoter methylation of DNA methyltransferases triggers DNA hypomethylation in human hepatocellular carcinoma (HepG2) cells. *Epigenetics*: 1-14.

Gibson, S.B., (2004). Epidermal growth factor and trail interactions in epithelial-derived cells. In *Vitamins & Hormones*. Academic Press. Vol. 67: 207-227

Grotto, D., Maria, L.S., Valentini, J., Paniz, C., Schmitt, G., Garcia, S.C., Pomblum, V.J., Rocha, J.B.T. and Farina, M., (2009). Importance of the lipid peroxidation biomarkers and methodological aspects for malondialdehyde quantification. *Quimica Nova*, *32*(1): 169-174.

Gruber-Dorninger, C., Novak, B., Nagl, V. and Berthiller, F., (2017). Emerging mycotoxins: Beyond traditionally determined food contaminants. Journal of agricultural and food chemistry, 65(33): 7052-7070.

Han, Z., Tangni, E.K., Huybrechts, B., Munaut, F., Scauflaire, J., Wu, A. and Callebaut, A., (2014). Screening survey of co-production of fusaric acid, fusarin C, and fumonisins B 1, B 2 and B 3 by Fusarium strains grown in maize grains. *Mycotoxin research*, *30*(4): 231-240.

Hardie, D.G., (2013). AMPK: a target for drugs and natural products with effects on both diabetes and cancer. *Diabetes*, *62*(7): 2164-2172.

Harmel, E., Grenier, E., Bendjoudi Ouadda, A., El Chebly, M., Ziv, E., Beaulieu, J.F., Sané, A., Spahis, S., Laville, M. and Levy, E., (2014). AMPK in the small intestine in normal and pathophysiological conditions. *Endocrinology*, *155*(3): 873-888.

Hastings, J.W. and Johnson, C.H., (2003). [3] Bioluminescence and chemiluminescence. In *Methods in enzymology*. Academic Press. Vol. 360: 75-104

Haupt, S., Berger, M., Goldberg, Z. and Haupt, Y., (2003). Apoptosis-the p53 network. *Journal of cell science*, *116*(20): 4077-4085.

Hodges, D.M., DeLong, J.M., Forney, C.F. and Prange, R.K., (1999). Improving the thiobarbituric acid-reactive-substances assay for estimating lipid peroxidation in plant tissues containing anthocyanin and other interfering compounds. *Planta*, *207*(4): 604-611.

Jaeschke, H., (2008). Toxic responses of the liver. *Casarett's & Doull's Toxicology: The Basic Science of Poisoning*: 557-582.

Jeon, S.M., (2016). Regulation and function of AMPK in physiology and diseases. *Experimental & molecular medicine*, *48*(7): 245.

Jiao, J., Sun, L., Zhou, B., Gao, Z., Hao, Y., Zhu, X. and Liang, Y., (2014). Hydrogen peroxide production and mitochondrial dysfunction contribute to the fusaric acid-induced programmed cell death in tobacco cells. *Journal of plant physiology*, *171*(13): 1197-1203.

Joerger, A.C. and Fersht, A.R., (2010). The tumor suppressor p53: from structures to drug discovery. *Cold Spring Harbor perspectives in biology*, *2*(6): 000919.

Kubista, M., Andrade, J.M., Bengtsson, M., Forootan, A., Jonák, J., Lind, K., Sindelka, R., Sjöback, R., Sjögreen, B., Strömbom, L. and Ståhlberg, A., (2006). The real-time polymerase chain reaction. *Molecular aspects of medicine*, *27*(2-3): 95-125.

Kaufmann, S.H., Lee, S.H., Meng, X.W., Loegering, D.A., Kottke, T.J., Henzing, A.J., Ruchaud, S., Samejima, K. and Earnshaw, W.C., (2008). Apoptosis-associated caspase activation assays. *Methods*, *44*(3): 262-272.

Kim, J., Yang, G., Kim, Y., Kim, J. and Ha, J., (2016). AMPK activators: mechanisms of action and physiological activities. *Experimental & molecular medicine*, *48*(4): 224.

Kim, S.H., Singh, M.P., Sharma, C. and Kang, S.C., (2018). Fumonisin B_1 actuates oxidative stress-associated colonic damage via apoptosis and autophagy activation in murine model. *Journal of biochemical and molecular toxicology*, *32*(7): 22161.

Kim, Y.M., HWANG, J.T., Kwak, D.W., Lee, Y.K. and Park, O.J., (2007). Involvement of AMPK signaling cascade in capsaicin-induced apoptosis of HT-29 colon cancer cells. *Annals of the New York Academy of Sciences*, *1095*(1): 496-503.

Kumar, P., Nagarajan, A. and Uchil, P.D., (2018). Analysis of cell viability by the lactate dehydrogenase assay. *Cold Spring Harbor Protocols*, *2018*(6): 095497.

Li, Y., Zhang, B., He, X., Cheng, W.H., Xu, W., Luo, Y., Liang, R., Luo, H. and Huang, K., (2014). Analysis of individual and combined effects of ochratoxin A and zearalenone on HepG2 and KK-1 cells with mathematical models. *Toxins*, *6*(4): 1177-1192.

Liu, B.H., Wu, T.S., Yu, F.Y. and Su, C.C., (2006). Induction of oxidative stress response by the mycotoxin patulin in mammalian cells. *Toxicological Sciences*, *95*(2): 340-347.

Liu, Y., Ao, X., Ding, W., Ponnusamy, M., Wu, W., Hao, X., Yu, W., Wang, Y., Li, P. and Wang, J., (2018). Critical role of FOXO3a in carcinogenesis. *Molecular cancer*, *17*(1): 104.

López-Díaz, C., Rahjoo, V., Sulyok, M., Ghionna, V., Martín-Vicente, A., Capilla, J., Di Pietro, A. and López-Berges, M.S., (2018). Fusaric acid contributes to virulence of Fusarium oxysporum on plant and mammalian hosts. *Molecular plant pathology*, *19*(2): 440-453.

López-Díaz, C., Rahjoo, V., Sulyok, M., Ghionna, V., Martín-Vicente, A., Capilla, J., Di Pietro, A. and López-Berges, M.S., (2018). Fusaric acid contributes to virulence of Fusarium oxysporum on plant and mammalian hosts. Molecular plant pathology: 440-453.

Mahmood, T. and Yang, P.C., (2012). Western blot: technique, theory, and trouble shooting. *North American journal of medical sciences*, *4*(9): 429.

Malladi, S., Challa-Malladi, M., Fearnhead, H.O. and Bratton, S.B., (2009). The Apaf-1• procaspase-9 apoptosome complex functions as a proteolytic-based molecular timer. *The EMBO journal*, *28*(13): 1916-1925.

Mathur, S., Constable, P.D., Eppley, R.M., Waggoner, A.L., Tumbleson, M.E. and Haschek, W.M., (2001). Fumonisin B1 is hepatotoxic and nephrotoxic in milk-fed calves. *Toxicological Sciences*, *60*(2): 385-396.

McStay, G.P. and Green, D.R., (2014). Measuring apoptosis: caspase inhibitors and activity assays. *Cold Spring Harbor Protocols*, *2014*(8): 070359.

McStay, G.P., Salvesen, G.S. and Green, D.R., (2008). Overlapping cleavage motif selectivity of caspases: implications for analysis of apoptotic pathways. *Cell death and differentiation*, *15*(2): 322.

Mehrotra, R.S., (2013). Fundamentals of Plant pathology. Tata McGraw-Hill Education.

Merrill Jr, A.H., Sullards, M.C., Wang, E., Voss, K.A. and Riley, R.T., (2001). Sphingolipid metabolism: roles in signal transduction and disruption by fumonisins. *Environmental health perspectives*, *109*(suppl 2): 283-289.

Mersch-Sundermann, V., Knasmüller, S., Wu, X.J., Darroudi, F. and Kassie, F., (2004). Use of a human-derived liver cell line for the detection of cytoprotective, antigenotoxic and cogenotoxic agents. *Toxicology*, *198*(1-3): 329-340.

Narváez Trujillo, E.A. and Portero Pico, C.E., (2015). Fusaric acid induces a notochord malformation in zebrafish via copper chelation.

O'brien, M, Moravec, R. and Riss, T., (2010). Caspase-glo™ 3/7 assay: use fewer cells and spend less time with this homogeneous assay. *Luminescence*, *200*

Ogata, S., Inoue, K., Iwata, K., Okumura, K. and TAGUCHI, H., (2001). Apoptosis induced by picolinic acid-related compounds in HL-60 cells. Bioscience, biotechnology, and biochemistry, 65(10): 2337-2339.

Parhamifar, L., Andersen, H. and Moghimi, S.M., (2013). Lactate dehydrogenase assay for assessment of polycation cytotoxicity. In *Nanotechnology for Nucleic Acid Delivery*. Humana Press, Totowa, NJ: 13-22

Paris, D.H., Richards, A.L. and Day, N.P., (2015). Orientia. In *Molecular Medical Microbiology*. Academic Press: 2057-2096

Park, S.M., Kim, S.W., Jung, E.H., Ko, H.L., Im, C.K., Lee, J.R., Byun, S.H., Ku, S.K., Kim, S.C., Park, C.A. and Kim, K.J., (2018). Sipjeondaebo-tang alleviates oxidative stress-mediated liver injury through activation of the CaMKK2-AMPK signaling pathway. *Evidence-Based Complementary and Alternative Medicine*, *2018*.

Patlevič, P., Vašková, J., Švorc Jr, P., Vaško, L. and Švorc, P., (2016). Reactive oxygen species and antioxidant defense in human gastrointestinal diseases. *Integrative medicine research*, *5*(4): 250-258.

Pavlovkin, J., Mistrik, I. and Prokop, M., (2004). Some aspects of the phytotoxic action of fusaric acid on primary Ricinus roots. *Plant Soil and Environment*, *50*(9): 397-401.

Pelosse, M., Cottet-Rousselle, C., Bidan, C.M., Dupont, A., Gupta, K., Berger, I. and Schlattner, U., (2019). Synthetic energy sensor AMPfret deciphers adenylate-dependent AMPK activation mechanism. *Nature communications*, *10*(1): 1038.

Pizzino, G., Irrera, N., Cucinotta, M., Pallio, G., Mannino, F., Arcoraci, V., Squadrito, F., Altavilla, D. and Bitto, A., (2017). Oxidative stress: harms and benefits for human health. *Oxidative Medicine and Cellular Longevity*, *2017*.

Pop, C., Salvesen, G.S. and Scott, F.L., (2008). Caspase assays: identifying caspase activity and substrates in vitro and in vivo. *Methods in enzymology*: 351-367.

Porter, A.G. and Jänicke, R.U., (1999). Emerging roles of caspase-3 in apoptosis. *Cell death and differentiation*, *6*(2): 99.

Qu, T., Huang, B., Zhang, L., Li, L., Xu, F., Huang, W., Li, C., Du, Y. and Zhang, G., (2014). Identification and functional characterization of two executioner caspases in Crassostrea gigas. *PloS one*, *9*(2): 89040.

Ramadori, G., Moriconi, F., Malik, I. and Dudas, J., (2008). Physiology and pathophysiology of liver inflammation, damage and repair. *J physiol Pharmacol*, *59*(Suppl 1): 107-117.

Rani, T.D., Savitha, R., Lavanya, L., Kamalalochani, S. and Bharathiraja, B., (2009). An overview of Fusaric acid production. *Advanced Biotech Mini Rev*: 18-22.

Rao, X., Lai, D. and Huang, X., (2013). A new method for quantitative real-time polymerase chain reaction data analysis. *Journal of Computational Biology*, *20*(9): 703-711.

Read, A.P. and Strachan, T., (1999). Chapter 18: Cancer Genetics. *Human molecular genetics*: *2.*

Reddy, R.V., Larson, C.A., Brimer, G.E., Frappier, B.L. and Reddy, C.S., (1996). Developmental toxic effects of fusaric acid in CD1 mice. *Bulletin of environmental contamination and toxicology*, *57*(3): 354-360.

Rehman, G., Shehzad, A., Khan, A.L. and Hamayun, M., (2014). Role of AMP-activated protein kinase in cancer therapy. *Archiv der Pharmazie*, *347*(7): 457-468.

Richter, E.A. and Ruderman, N.B., (2009). AMPK and the biochemistry of exercise: implications for human health and disease. *Biochemical Journal*, *418*(2): 261-275.

Riss, T.L., Moravec, R.A., Niles, A.L., Duellman, S., Benink, H.A., Worzella, T.J. and Minor, L., (2016). Cell viability assays. In *Assay Guidance Manual [Internet]*. Eli Lilly & Company and the National Center for Advancing Translational Sciences.

Riss, T, O'brien, M. and Moravec, R., (2003). Choosing the right cell-based assay for your research. *Cell notes*, *6*(1): 6.

Rong, X., Sun-Waterhouse, D., Wang, D., Jiang, Y., Li, F., Chen, Y., Zhao, S. and Li, D., (2019). The Significance of Regulatory MicroRNAs: Their Roles in Toxicodynamics of Mycotoxins and in the Protection Offered by Dietary Therapeutics Against Mycotoxin-Induced Toxicity. *Comprehensive Reviews in Food Science and Food Safety*, *18*(1): 48-66.

Salvesen, G.S. and Walsh, C.M., (2014), June. Functions of caspase 8: the identified and the mysterious. In *Seminars in immunology*. Academic Press. Vol. 26, No. 3: 246-252.

Sanli, T., Steinberg, G.R., Singh, G. and Tsakiridis, T., (2014). AMP-activated protein kinase (AMPK) beyond metabolism: a novel genomic stress sensor participating in the DNA damage response pathway. *Cancer biology & therapy*, *15*(2): 156-169.

Scabini, M., Stellari, F., Cappella, P., Rizzitano, S., Texido, G. and Pesenti, E., (2011). In vivo imaging of early stage apoptosis by measuring real-time caspase-3/7 activation. *Apoptosis*, *16*(2): 198-207.

Schaich, K.M., (2016). Analysis of lipid and protein oxidation in fats, oils, and foods. In *Oxidative stability and shelf life of foods containing oils and fats*. AOCS Press: 1-131

Schieber, M. and Chandel, N.S., (2014). ROS function in redox signaling and oxidative stress. *Current biology*, *24*(10): 453-R462.

Seervi, M. and Xue, D., (2015). Mitochondrial cell death pathways in Caenorhabiditis elegans. In *Current topics in developmental biology*. Academic Press. Vol. 114: 43-65.

Shamas-Din, A., Brahmbhatt, H., Leber, B. and Andrews, D.W., (2011). BH3-only proteins: Orchestrators of apoptosis. *Biochimica et Biophysica Acta (BBA)-Molecular Cell Research*, *1813*(4): 508-520.

Shukla, S., Saxena, S., Singh, B.K. and Kakkar, P., (2017). BH3-only protein BIM: An emerging target in chemotherapy. *European journal of cell biology*: 728-738.

Sies, H., 1993. Strategies of antioxidant defense. *European journal of biochemistry*, *215*(2): 213-219.

Singh, M.P. and Kang, S.C., (2017). Endoplasmic reticulum stress-mediated autophagy activation attenuates fumonisin B1 induced hepatotoxicity in vitro and in vivo. *Food and Chemical Toxicology*, *110*: 371-382.

Singh, V.K. and Upadhyay, R.S., (2014). Fusaric acid induced cell death and changes in oxidative metabolism of Solanum lycopersicum L. *Botanical studies*, *55*(1): 66.

Singh, V.K. and Upadhyay, R.S., 2016, December. Induction of defence response by fusaric acid (Fusarium toxin) in tomato plant. In *6th International conference on agriculture, environment and biological sciences* (pp. 1-22).

Souza, D.M.B., Barros, M.G.O., Silva, J.S.C., Silva, M.B., Coleto, Z.F., Jimenez, G.C., Adrião, M. and Wischral, A., (2012). Detection of mutations within exons 4 to 8 of the p53 tumor suppressor gene in canine mammary glands. *Arquivo Brasileiro de Medicina Veterinária e Zootecnia*, *64*(2): 341-348.

Stack, B.C., Ye, J., Willis, R., Hubbard, M. and Hendrickson, H.P., (2014). Determination of oral bioavailability of fusaric acid in male Sprague-Dawley rats. Drugs in R&d, 14(2): 139-145.

Stockmann-Juvala, H., Mikkola, J., Naarala, J., Loikkanen, J., Elovaara, E. and Savolainen, K., (2004). Fumonisin B1-induced toxicity and oxidative damage in U-118MG glioblastoma cells. *Toxicology*, *202*(3): 173-183.

Stockmann-Juvala, H. and Savolainen, K., (2008). A review of the toxic effects and mechanisms of action of fumonisin B1. *Human & experimental toxicology*, *27*(11): 799-809.

Su, D., Wang, X., Campbell, M.R., Song, L., Safi, A., Crawford, G.E. and Bell, D.A., (2015). Interactions of chromatin context, binding site sequence content, and sequence evolution in stress-induced p53 occupancy and transactivation. *PLoS genetics*, *11*(1): 1004885.

Temmerman, R., Scheirlinck, I., Huys, G. and Swings, J., (2003). Culture-independent analysis of probiotic products by denaturing gradient gel electrophoresis. *Appl. Environ. Microbiol.*, *69*(1): 220-226.

Venkatesh, N. and Keller, N.P., (2019). Mycotoxins in conversation with bacteria and fungi. *Frontiers in microbiology*: *10*.

Voss, K.A., Plattner, R.D., Bacon, C.W. and Norred, W.P., (1990). Comparative studies of hepatotoxicity and fumonisin B 1 and B 2 content of water and chloroform/methanol extracts of Fusarium moniliforme strain MRC 826 culture material. *Mycopathologia*, *112*(2): 81-92.

Voss, K.A., Smith, G.W. and Haschek, W.M., (2007). Fumonisins: toxicokinetics, mechanism of action and toxicity. *Animal feed science and technology*, *137*(3-4): 299-325.

Voss, K.A. and Riley, R.T., (2013). Fumonisin toxicity and mechanism of action: overview and current perspectives. *Food Safety*, *1*(1): 2013006-2013006.

Walsh, J.G., Cullen, S.P., Sheridan, C., Lüthi, A.U., Gerner, C. and Martin, S.J., (2008). Executioner caspase-3 and caspase-7 are functionally distinct proteases. *Proceedings of the National Academy of Sciences*, *105*(35): 12815-12819.

Wang, X., Hu, S. and Liu, L., (2017). Phosphorylation and acetylation modifications of FOXO3a: Independently or synergistically?. *Oncology letters*, *13*(5): 2867-2872.

Wu, Y., Li, T., Gong, L., Wang, Y. and Jiang, Y., (2019). Effects of Different Carbon Sources on Fumonisin Production and FUM Gene Expression by Fusarium proliferatum. *Toxins*, *11*(5): 289.

Yamada, S., Nakamura, H., Kinoshita, E., Kinoshita-Kikuta, E., Koike, T. and Shiro, Y., (2007). Separation of a phosphorylated histidine protein using phosphate aYnity polyacrylamide gel electrophoresis. *Analytical biochemistry*, *360*: 160-162.

Yao, S., Fan, L.Y.N. and Lam, E.W.F., (2018), June. The FOXO3-FOXM1 axis: A key cancer drug target and a modulator of cancer drug resistance. In *Seminars in cancer biology*. Academic Press. Vol. 50: 77-89.

Yin, E.S., Rakhmankulova, M., Kucera, K., de Sena Filho, J.G., Portero, C.E., Narváez-Trujillo, A., Holley, S.A. and Strobel, S.A., (2015). Fusaric acid induces a notochord malformation in zebrafish via copper chelation. *BioMetals*, *28*(4): 783-789.

Yuan, Q., Jiang, Y., Fan, Y., Ma, Y., Lei, H. and Su, J., (2019). Fumonisin B1 Induces Oxidative Stress and Breaks Barrier Functions in Pig Iliac Endothelium Cells. *Toxins*, *11*(7): 387.

Yun, H., Park, S., Kim, M.J., Yang, W.K., Im, D.U., Yang, K.R., Hong, J., Choe, W., Kang, I., Kim, S.S. and Ha, J., (2014). AMP-activated protein kinase mediates the antioxidant effects of resveratrol through regulation of the transcription factor FoxO1. *The FEBS journal*, *281*(19): 4421-4438.

Zadra, G., Batista, J.L. and Loda, M., (2015). Dissecting the dual role of AMPK in cancer: from experimental to human studies. *Molecular cancer research*, *13*(7): 1059-1072.

Zain, M.E., (2011). Impact of mycotoxins on humans and animals. *Journal of Saudi Chemical Society*, *15*(2): 129-144.

Zamaraeva, M.V., Sabirov, R.Z., Maeno, E., Ando-Akatsuka, Y., Bessonova, S.V. and Okada, Y., (2005). Cells die with increased cytosolic ATP during apoptosis: a bioluminescence study with intracellular luciferase. *Cell death and differentiation*, *12*(11): 1390.

Zhou, B., Ho, S.S., Greer, S.U., Spies, N., Bell, J.M., Zhang, X., Zhu, X., Arthur, J.G., Byeon, S., Pattni, R. and Saha, I., (2019). Haplotype-resolved and integrated genome analysis of the cancer cell line HepG2. *Nucleic acids research*, *47*(8): 3846-3861.

Zmijewski, J.W., Banerjee, S., Bae, H., Friggeri, A., Lazarowski, E.R. and Abraham, E., (2010). Exposure to hydrogen peroxide induces oxidation and activation of AMP-activated protein kinase. *Journal of Biological Chemistry*, *285*(43): 33154-33164.

APPENDICES

APPENDIX A

Bicinchoninic Acid (BCA) Assay

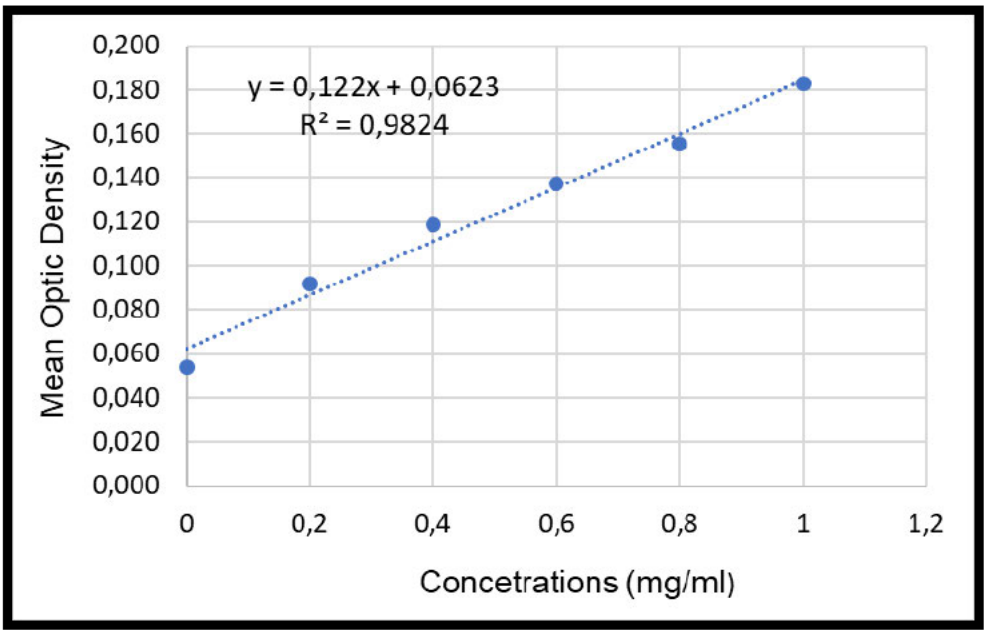

Fig5. 1: Standard curve demonstrating known concentrations of bovine serum albumin (BSA) used to determine the concentration of protein present in each sample.

Table 4. 1: Standardisation of proteins (Final volume = 350µl; Concentration = 1.0mg/ml)

Sample	Mean Absorbance	Protein Concentration (mg/ml)	Volume of Protein Stock (µl)	Volume of Cytobuster (µl)	Volume of Laemmli Buffer (µl)
Control	0,372	2,5344	79	121	50
5µM	0,349	2,3459	85	115	50
27µM	0,312	2,0467	98	102	50
100µM	0,232	1,3869	144	56	50
Combined IC_{50}s	0,219	1,2803	156	44	50

APPENDIX B

Real-time quantitative PCR (qPCR)

Expressions of miR124

FA and FB_1 regulated the expressions of miR124 in HepG2 cells (*p<0.0001*).

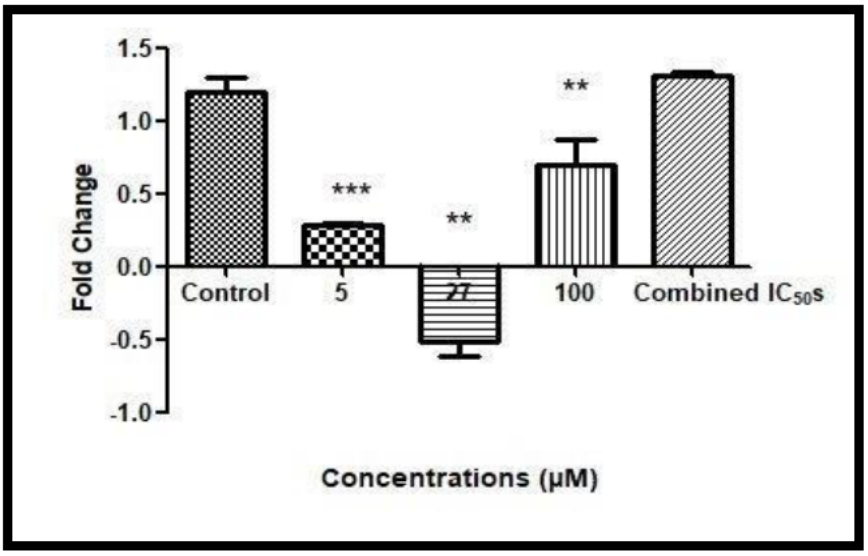

Fig5. 2: FA and FB_1 significantly downregulated the expressions of miR124 at 5µM, 27µM and 100µM. At combined IC_{50}s the expression was increased.